Chapter 3
Geology and Geomorphology of Azokh Caves

Patricio Domínguez-Alonso, Enrique Aracil, Jose Angel Porres, Peter Andrews, Edward P. Lynch, and John Murray

Abstract Azokh Cave is located in the Lesser Caucasus and is hosted in Mesozoic limestone. It comprises a series of karstic cavities, chambers and passageways that interconnect to form a larger cave network, the trend of which appears to have been influenced by fracture patterns in the bedrock. The geomorphology of the currently accessible areas of the cave is presented, with many of its speleological features described in detail for the first time. Electrical resistivity tomography is used to examine variation in thickness of sediments infilling the inner chambers of the cave. This information, coupled with data relating to the surface topography of the cave infill, sheds light on patterns of sediment deposition within the cave system. It remains unclear whether the cave formed from epigenic or hypogenic speleological processes (or a combination of the two). This question is further hampered by the presence of a large bat population in the interior of the cave, the guano deposits of which have modified the inner galleries.

Резюме Полное и детальное описание геоморфологии пещерной системы Азоха представлено здесь впервые. Пещера сформировалась в богатой карстовой сети мезозойского известняка и состоит из четырех больших внутренних камер (помеченных как галереи Азоха *I–IV*), которые латерально связаны между собой и расположены в направлении от северо-запада на юго-восток. С внешним миром камеры связаны посредством ряда перпендикулярно выходящих проходов (*Азох 1, 5* и *6*). Эти пещерные каналы имеют одинаковую ориентацию с региональной особенностью соединения на уровне бедрока. В геоморфологии пещеры явно заметны признаки карстового провала. В одном из "слепых" внешних проходов (*Азох 2*) доступ к внутренним галереям заблокирован. Образование черта (сланца) в известняке имело обратный эффект: на местах он укреплял и поддерживал структуры потолка, помогая сохранить различные камеры пещеры. На перекрестной топографии пещеры заметна высокая центральная зона (между внутренними камерами *Азох 2* и *Азох 3*) с уклоном в сторону двух концов пещерной системы, хотя это снижение несколько более выражено по направлению к проходу *Азох 1*.

Толщина седиментного слоя в различных камерах пещеры определена геофизическим методом – вычислением удельного электрического сопротивления. Этот подход позволяет картировать заполненную толщину внутри пещеры, и эта величина варьирует в пределах от <1 м до 3 м+. Максимальная толщина седимента отмечена в камере *Азох 1*, хотя участки с большой толщиной встречаются и у входа в *Азох 2*, а также в более центральных местах камер *Азох 2, 3* и *4*. С помощью компьютерной программы *Surfer* была вычислена площадь поверхности (примерно 1,390 м^2) большого объема седимента (около 1,367 м^3), лежащего на известняковом бедроке во внутренних галереях Азохской пещеры.

Patricio Domínguez-Alonso – Deceased

P. Domínguez-Alonso
Departamento de Paleontología, Facultad de Ciencias Geologicas & Instituto de Geociencias (IGEO-CSIC), Universidad Complutense de Madrid (UCM), Madrid, Spain

E. Aracil
Análisis y Gestión del Subsuelo, S.L. (AGS), c/Luxemburgo, 4; Oficina 3; E-28224-Pozuelo de Alarcón, Madrid, Spain
e-mail: e.aracil@ags-geofisica.com

E. Aracil · J.A. Porres
Departamento de Geodinámica. Facultad Ciencias Geológicas., Universidad Complutense de Madrid (UCM), c/ José Antonio Novais n. 12, 28040 Madrid, Spain
e-mail: japorres@ubu.es

P. Andrews
Natural History Museum, Cromwell Road, London, SW7 5BD, UK
e-mail: pjandrews@uwclub.net

E.P. Lynch · J. Murray (✉)
Earth & Ocean Sciences, School of Natural Sciences, National University of Ireland, Galway, University Road, Galway, Ireland
e-mail: john.murray@nuigalway.ie

E.P. Lynch
e-mail: Edward.lynch@nuigalway.ie

Yolanda Fernández-Jalvo et al. (eds.), *Azokh Cave and the Transcaucasian Corridor*, Vertebrate Paleobiology and Paleoanthropology, DOI 10.1007/978-3-319-24924-7_3

Геофизические профили выявляют также различные аномалии внутри известняка, которые, судя по их морфологии и величинам удельного сопротивления, возможно, представляют собой полости в бедроке, заполненные, как правило, мелкозернистым материалом. Все обнаруженные полости обычно ассоциированы с аномалиями проводимости в профилях, причинами которых являются разломы. Это подтверждает взаимосвязь между развитием разлома, образованием карстового рельефа и формированием полостей.

Остается неясным, сформировалась ли Азохская пещера под воздействием поверхностных вод, уходящих в почву и растворяющих нижележащий известковый бедрок (эпигенетический спелеогенез), или альтернативно, т.е. поднимающейся снизу водой, растворяющей горную породу (гипогенетичесский спелеогенез). Возможно также сочетанное влияние этих двух процессов. Рассматриваемая проблема усложняется из-за наличия большой колонии летучих мышей в пещерной системе. Толстые отложения гуано, выработанные этими существами, в некоторых направлениях изменили (и продолжают изменять) поверхность внутренних галерей.

Keywords Lesser Caucasus • Limestone • Karstic • Electrical resistivity • Epigenic • Hypogenic

Introduction

Azokh Cave is located at the southern end of the Lesser Caucasus at 39° 37.15′ north and 46° 59.32′ east (Fig. 3.1). The wider region surrounding the site effectively marks the boundary between Europe and Asia. Both the Lesser and Greater Caucasus (positioned further north; see Fig. 3.1c) run broadly parallel to each other and formed during the Himalayan-Alpine orogeny in Late Mesozoic to Cenozoic times. These two mountain ranges cross the Caucasian isthmus between the Black and Caspian seas and they are separated by the intermontane Kura Basin, which contains Paleogene to Quaternary molasse sediments.

The cave is part of a much larger karst network developed in Mesozoic limestone, which is now abandoned. It contains an appreciable amount of sediment infill and, as it is presently home to one of the largest bat populations in the Southern Caucasus, thick deposits of guano are present in the interior.

Murray et al. (2010) recently described between 11 and 12 m of sediments infilling the largest of the entrance passages to the cave [Azokh 1]. This particular passage had been extensively excavated in the past by a Soviet-Azeri team (Huseinov 1985; Ljubin and Bosinski 1995; Lioubine 2002) and the stratigraphy remaining is split between two sedimentary sequences, which are no longer physically connected. The lower (and presumably oldest) of the two sequences is very limited in extent and has produced very few fossils; however, the upper sequence, preserved at the rear of the passage, has produced abundant fossil specimens, including numerous types of macro- and micro-mammals (Fernández-Jalvo et al. 2010). The base of the upper sequence is dated between 200 and 300 ka (i.e. Middle Pleistocene), whilst the uppermost horizon is Holocene. The actual Pleistocene-Holocene transition is apparently not preserved and is marked by an erosional disconformity (Murray et al. 2010, 2016).

Azokh Cave is significant from a paleoanthropological perspective for three reasons. Firstly, it is geographically located at an important migratory route-way between the African subcontinent and Eurasia (Fernández-Jalvo et al. 2010); secondly, middle-Pleistocene hominin remains were recovered from Azokh 1 passage during the previous phase of excavation work (Kasimova 2001); and thirdly, the presently available evidence shows that the cave contains a long sedimentary sequence recording different phases of occupation by three different hominin groups (King et al. 2016).

The purpose of this contribution is to provide a review of the geology and geomorphology of Azokh Cave. Understanding the intricacies of the cave system is crucial in helping us interpret how humans and animals may have utilized it as a shelter in the past. Both topographic and geophysical surveying techniques have been employed for this purpose. The former approach examines the shape and form of cave development between the surface of the sediment infill and the cave ceiling. This represents the space one can presently walk through and will be described first. Geophysics allows visualization of the cave system beneath ground-level and, in particular, it is quite effective at resolving the space between the surface of the infill and the rocky floor of the cave beneath, in addition to highlighting any buried (open) cavities.

Geological Background

The Caucasus Mountains were produced during tectonic collision between the Arabian and Eurasian plates, which resulted in the closure of the Tethyan Ocean during Mesozoic and Cenozoic times (Saintoti et al. 2006). As a result, the regional geology is dominated by sedimentary (typically carbonates) and volcanic rocks (Fig. 3.2; see also Fig. 3.1b, c), which have subsequently been subjected to varying degrees of folding and thrusting.

Subduction of the ocean floor of, what has been termed, the *Neo*tethys is believed to have possibly initiated during the Jurassic. Volcanic arcs and back-arc basins formed during the Late Jurassic and Cretaceous, while in the Late Cretaceous and (particularly) early Cenozoic, compressional deformation,

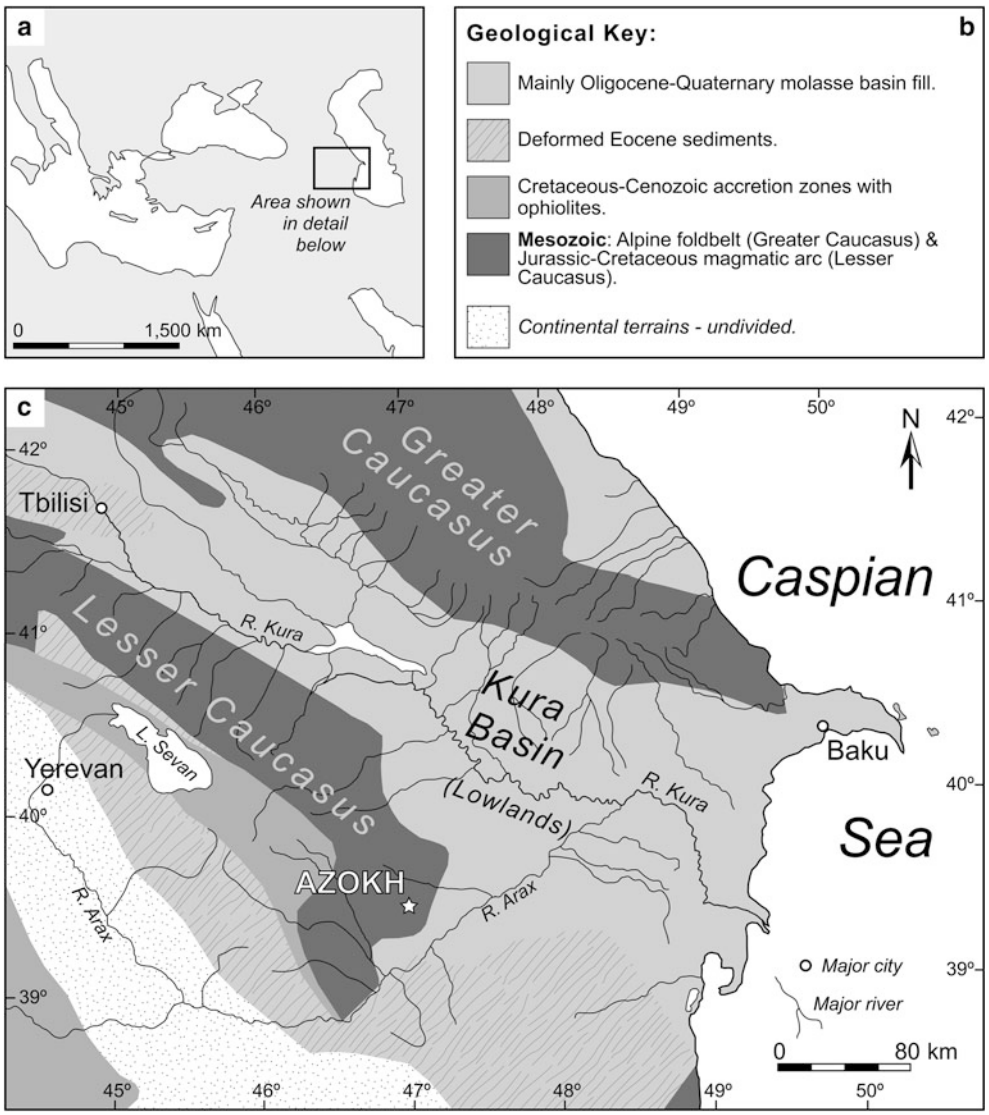

Fig. 3.1 Regional geological setting of Azokh Cave. **a** General geography of the wider region showing location (inset) of geological map in (**c**); **b** Key to geological map in (**c**); **c** Simplified geological map of the Southern Caucasus, with the location of Azokh Cave shown with a white star. Reproduced from Murray et al. (2010). Geographic and hydrographic information has been sourced from UN Map no. 3761, Revision 6, 2007. Geological information has been adopted and modified from that of Brunet et al. (2003)

basin inversion and subduction- to collision-related magmatism were characteristic of the region (Sosson et al. 2010; Dilek et al. 2009). The compressional tectonic regime generated by this collision resulted in uplift of the Caucasian mountain ranges and these have continued to rise since Miocene times (Egan et al. 2009). Mosar et al. (2010) note that the average (annual) convergence of the Arabian and Eurasian plates is on the order of 18–23 mm, resulting in tectonic activity (earthquakes) continuing to affect the wider region (see for example Karakhanian et al. 2004; Mellors et al. 2012).

Karst development, leading to the formation of the Azokh Cave system, took place in this geomorphologically and tectonically dynamic environment, presumably in mid to late Cenozoic times. The landscape surrounding the cave-site is mountainous (particularly towards the west) and deeply carved valleys and abandoned river terraces testify to rapid lowering of the base level in the past, which forced fluvial incision and deactivated endokarst systems.

Azokh Cave is developed in thickly bedded Mesozoic limestones, which are pale gray and commonly display a variety of textures, ranging from wackestone to grainstone. A significant level of partial or complete silicification, including development of conspicuous chert horizons, is often observed. Throughout the limestone sequence hosting the cave, these siliceous masses (which may be metric to decimetric in scale) have played an important role in controlling the formation of cavities and in the stabilization of roofs and vaults.

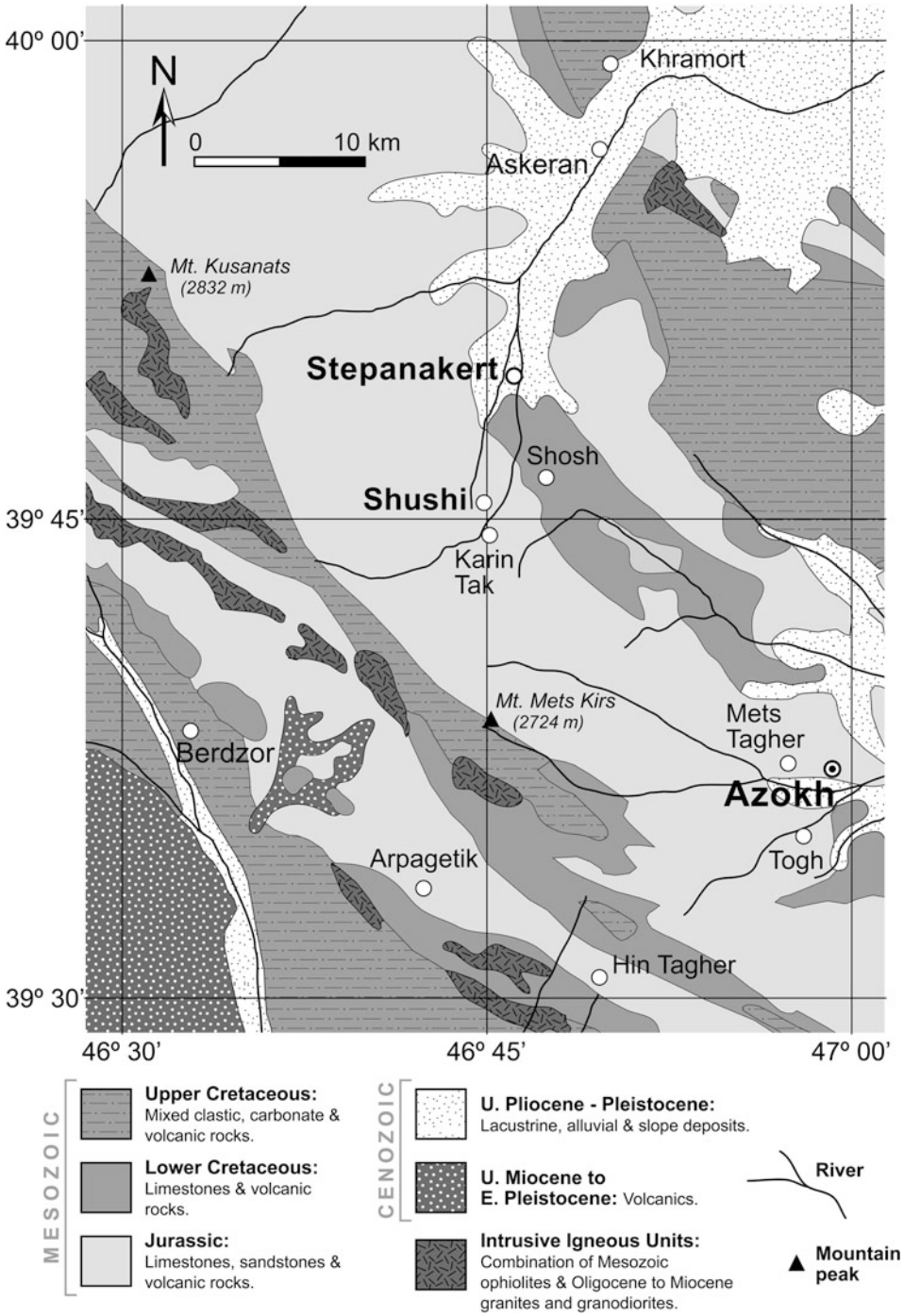

Fig. 3.2 Mesozoic to Cenozoic geology of the area surrounding Stepanakert and Azokh. Simplified from Vardanyan et al. (2010)

Marine fossils have been recovered from the limestone (Fig. 3.3a–c). Samples of silicified sponge and both open branching (dendroid) and massive scleractinian corals have been collected from outcrops in the vicinity of the cave. Very conspicuous *Thalassinoides*-type fossil burrows are evident in the bedrock at the main entranceway to Azokh Cave (Fig. 3.3d). This ichnofossil is characterized by a series of fairly large diameter tubes (20–40 mm at Azokh), which branch in a complex manner, leading to development of a 3-dimensional network. These burrows typically form in reasonably shallow, open shelf settings. Crucially, the burrow network has been pervasively silicified (presumably due to the infilling sediment having a more favorable porosity for percolating silica-rich fluids), resulting in a strong interconnected barrier to karstic solution. In places along the cave wall where the host limestone has been dissolved away, sandy/silty cave-filling sediments are observed infilling the

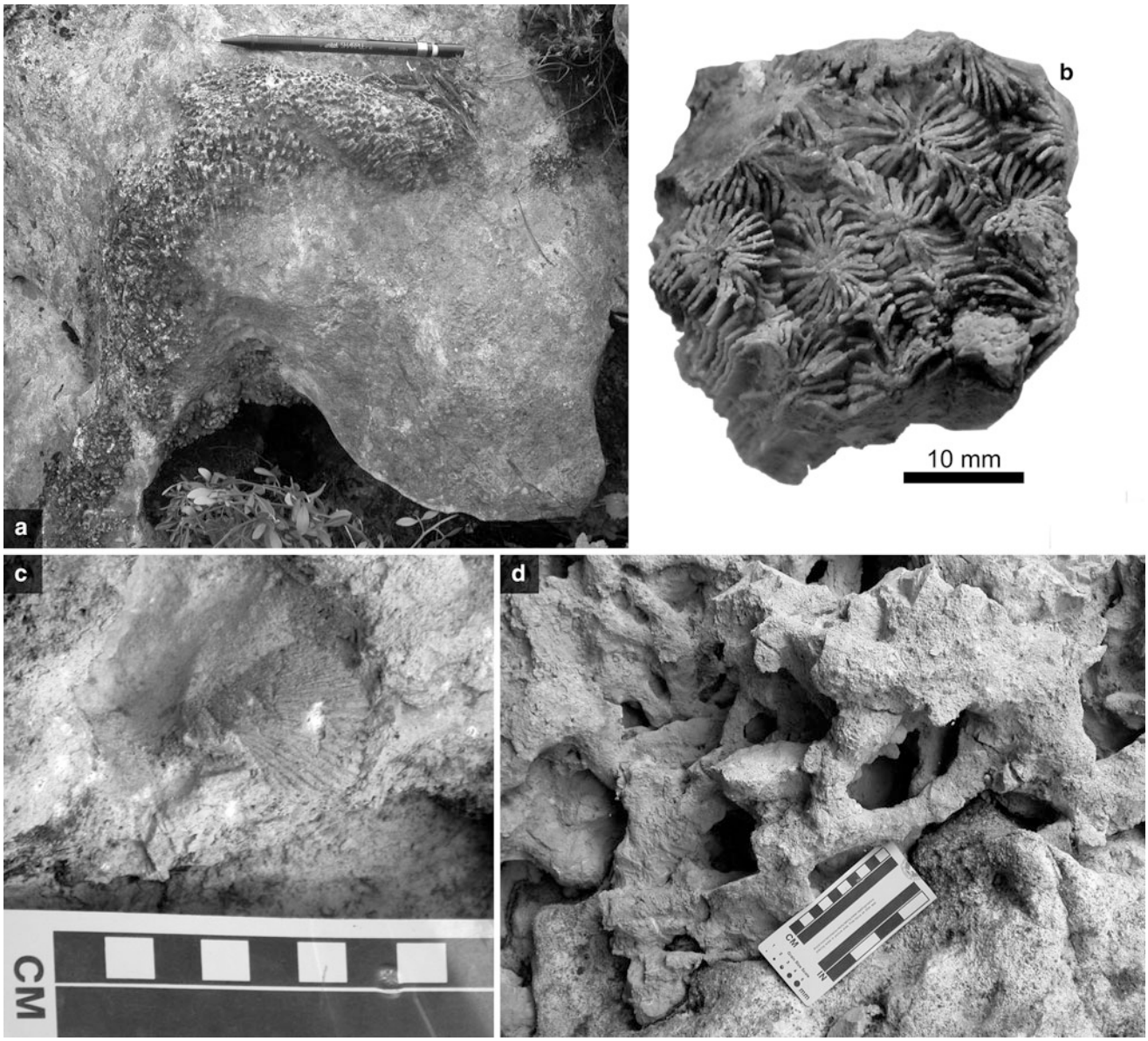

Fig. 3.3 Mesozoic fossils from the limestone at Azokh. **a** Silicified colonial coral weathering proud of the limestone matrix (pencil for scale); **b** Detail of a silicified colonial coral (found loose). Note in some instances the septa are confluent; **c** Valve of a marine shell *in-situ* in the wall of Azokh 1 passage; **d** Silicified *Thalassinoides*-type burrow network (basal trench, Azokh 1 passage)

interstitial areas between the silicified burrows; however, in some instances buff-yellow clays drape these spaces.

The precise age of the cave bedrock is still uncertain. Lioubine (2002) states that the cave is located on the calcareous massif of the Jurassic. This certainly seems to fit, in a broad sense, with descriptions of the wider regional geology (Fig. 3.2). The best hope of fixing an absolute age for the cave's host bedrock will perhaps come from a thick volcaniclastic interval found interbedded with the limestone 2 km to the west of the cave site. Murray et al. (2010) reported reworked (detrital) fine-grained igneous material interspersed in some of the sedimentary infill at Azokh Cave.

Geomorphology of Azokh Cave

Azokh Cave is located about 1 km to the east of a nearby village with the same name. The cave system is developed in a hillside on the eastern side of a small (broadly north-south trending) valley (Fig. 3.4). The bedrock at the site forms a prominent NNW-SSE trending escarpment (Fig. 3.5), which is west facing and divisible into two very thick carbonate units (termed *Lower* and *Upper Limestone [Lst.] Units* on Fig. 3.5a). Several different cave entrances are present in the *Lower Limestone Unit*. Locally the bedding in the limestone appears to be orientated horizontally; however, it is in fact

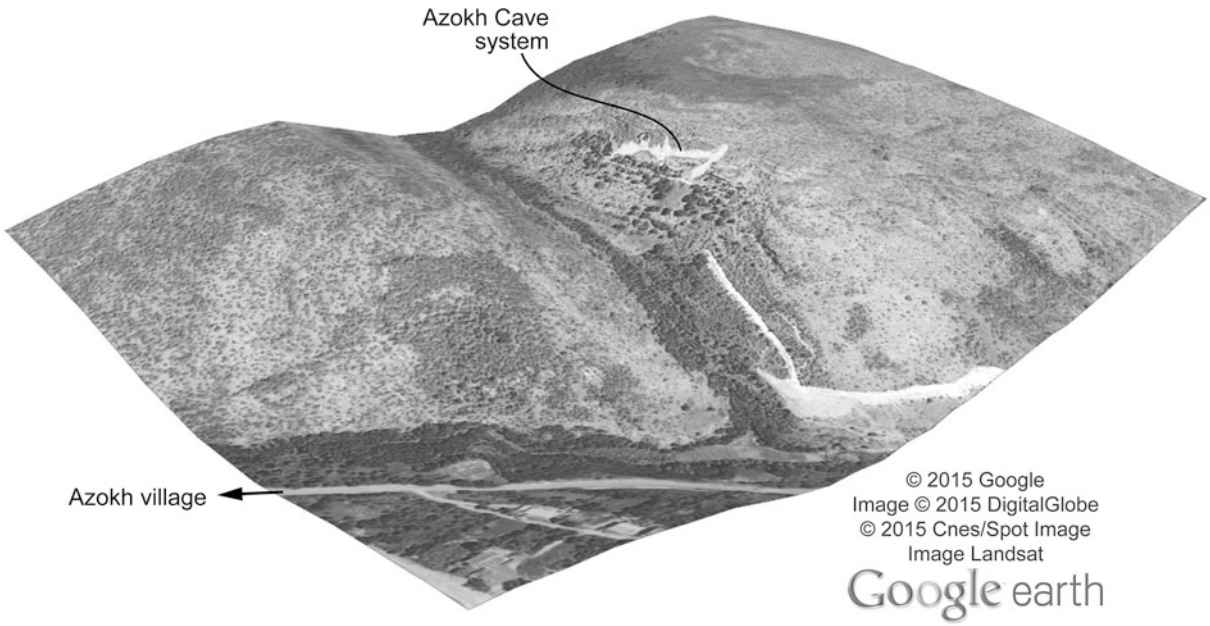

Fig. 3.4 Oblique 3-d view (looking towards the northeast) of the hillside hosting the Azokh Cave system (shown in white). The road in the foreground runs into the center of Azokh Village. Sourced from Google Earth

very gently folded on a larger scale, with the axis of the resultant anticline orientated broadly perpendicular to the escarpment.

When traversing through the interior of the cave, most of the chambers are carved through the lowermost part of the *Upper Limestone Unit*. However, detailed survey work, presented below, has shown cave galleries to be developed also in at least the uppermost part of the *Lower Limestone Unit*. A series of vertical shafts (cupolas) penetrate the uppermost part of the *Upper Limestone Unit*, breaking out at the surface in one open pit and also a collapse doline (see Fig. 3.5a, c). The cave-hosting limestone escarpment is actually truncated at either end by two large collapse features (Fig. 3.5a).

The bedrock hosting the cave system at Azokh displays pervasive fracturing and jointing (Fig. 3.6). Strongly developed vertical and horizontal joint sets occur throughout the limestone and appear to have played an influential role in the development of the karst system. Joints represent discrete brittle extensional fractures within bedrock where there has been little or no displacement along the plane of fracture (e.g., Fossen 2010). They develop during uplift, cooling, shrinkage and decompression of the rock unit, and joint orientations are principally controlled by the direction of regional and tectonic deformational stresses, combined with the mineralogical and mechanical properties of the host rock (e.g., Narr and Suppe 1991; Gross et al. 1995). Sub-aerial weathering and erosion (enhanced by percolating groundwater) can accentuate the development of joint sets and fracture systems.

Limestone joint mapping was carried out in the vicinity of Azokh Cave in order to identify the types of jointing present, to find the number of joint sets, to quantify the 3-dimensional orientation of the fractures (with respect to geographic north) and to establish spatial and genetic relationships between the jointing and the main cave system. Joint azimuths (0°–360°) and dips (0°–90°) were recorded along a linear traverse that ran along the upper ledge of the NNW-SSE limestone escarpment. In total, nine measurement stations were established, at 30 m spacing, and their positions recorded using GPS. Joint exposure varied along the traverse; however, individual measurements on both vertical and horizontal joint planes were made during the exercise. The results of part of this dataset (n = 171) are presented in Fig. 3.7, which shows the orientation of sub-vertical joint sets for each mapping station in the form of directional rose diagrams created using Stereonet 9.5 (Cardozo and Allmendinger 2013).

The directional data for the sub-vertical joints indicates that two principal joint orientations, approximately toward the NE and NW, are developed in the limestone. Field observations suggest that both joint sets are contemporaneous and comprised of systematic, regular extensional fractures. The most common joint set is a NE to ENE coaxial set, although this observation may be due to its preferential exposure along the traversed NNW-aligned escarpment (Fig. 3.7). Overall, the measured orientations define a conjugate joint system of sub-parallel fracture sets that remains broadly consistent between the measurement stations, particularly in the immediate vicinity of Azokh Cave. Joint sets

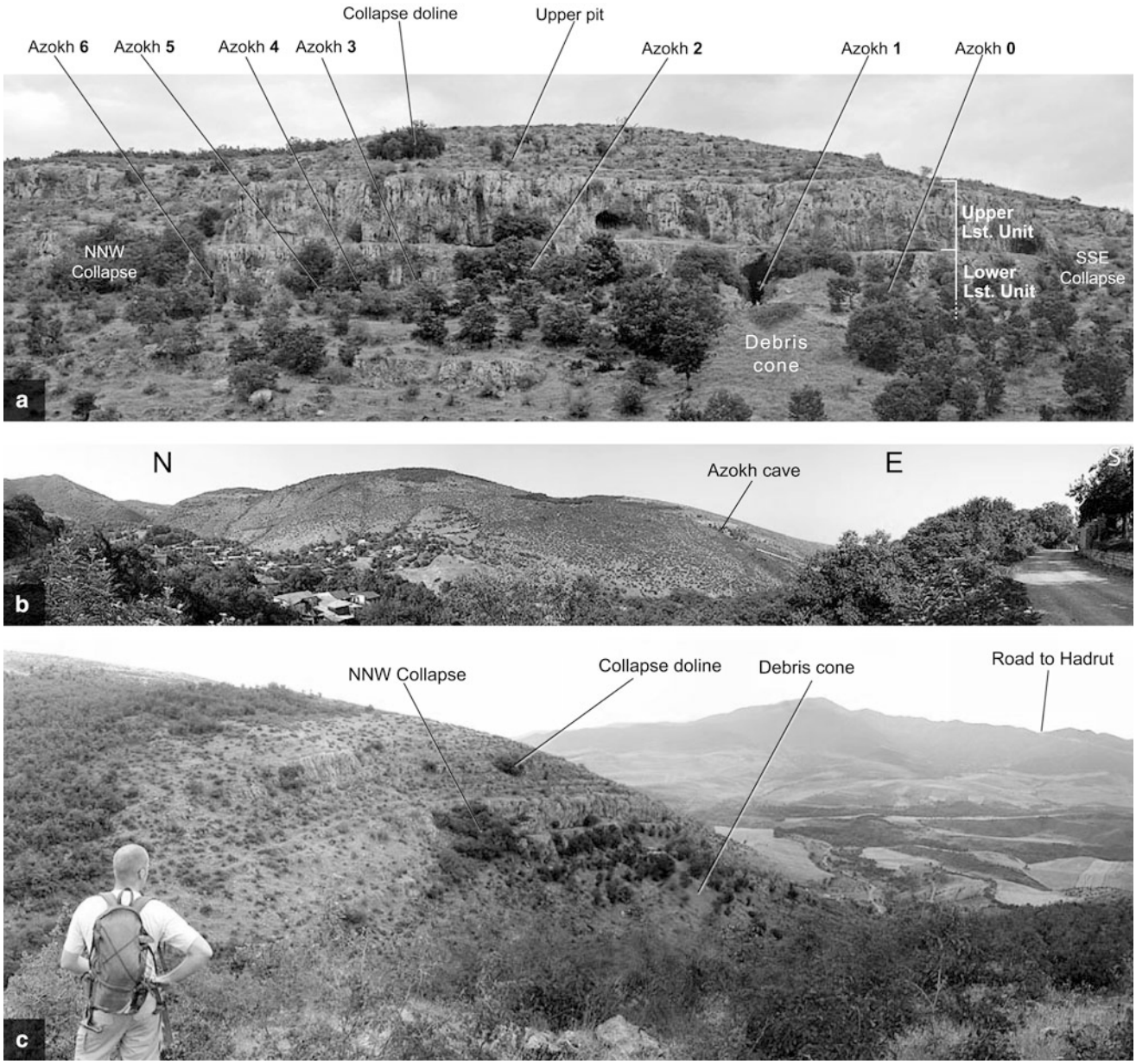

Fig. 3.5 External views of the Azokh Cave system. **a** Field photograph of the west-facing hillside containing the various entrances to the cave. Local visitors to the site would normally enter through Azokh 1 and exit through Azokh 6. Azokh 5 is a recently discovered entrance passage and Azokh 2 is a small gallery blocked by a choke. This blockage can be seen from the upper pit (labeled) and a collapse doline is marked by a small dense thicket of trees. Azokh 0 is a 3 m long narrow (and low) pass. The *Upper* and *Lower Limestone (Lst.) Units*, in which the cave system is developed, are clearly indicated in the cliff section. The intersection between these two units is stepped back and marked by a walkway. The continuous limestone cliff section is truncated at either end by two (NNW and SSE) collapsed dolines; **b** General landscape panorama from the top of Azokh village (taken around the area of the school); **c** General view southwards from the valley in which Azokh Cave opens

that deviate from the general NE and NW alignment are generally located furthest from the cave system. These 'distal' sets have a more NNE and WNW orientation and maintain a conjugate nature, albeit with a larger dihedral angle (Fig. 3.7).

The joint orientation data broadly corresponds with the alignment of various linear features seen across the cave system, such as passageways and elongate chambers. This association is particularly developed along a NE-SW direction. Likewise, the four inner chambers of the cave (Azokh I

Fig. 3.6 Example of sub-vertical and sub-horizontal joints in the limestone bedrock close to Azokh Cave. Hammer (circled) for scale

to IV; Fig. 3.8), if considered as a single broad lineament, also appear to be aligned sub-parallel to the broadly NW-orientated joint sets mapped in Fig. 3.7. This concordance suggests that joint formation, in response to local and/or regional stress fields, had an influence on subsequent karst development and cave morphology.

Materials and Methods of the Topographic Survey

This survey was completed over several field-seasons, to an accuracy of grade 5D according to the standards of the British Cave Research Association (Day 2002), although most of the internal survey within the cave was conducted at grade 6. Grade 5 is accomplished if compass and clinometer readings are accurate to ±1° (with ±0.5° used in practice) and the error in spatial positioning of the base-stations is ±10 cm. The compass and clinometer used for the survey work both need to be calibrated locally and immediately before and after the surveying. Measurements were always taken to the next base-station and then in reverse from the previous. Class D implies that additional measurements of cave passage profile were taken at survey stations and also wherever else needed.

Bearing and elevation were measured with precision compasses and clinometers [*Silva Sight Master Compass SM 360* and *Silva Clino Master Clinometer CM 360*, both PA (surveys 2004–2005) and LA series (2006 and later surveys)]. Distances were measured with a 50 m low-stretch tape. Additional measurements were taken using a 10 m retractable tape and distance to inaccessible areas (such as points along the ceiling or deepness of pits) was recorded using laser rangefinders. Magnetic north was consistently used during survey work.

In 2002 a general rough plan of the cave system was made at grade 3. In 2004, a preliminary survey to grade 4B was conducted to record the general profile of the ground surface within the cave. In 2005, this ground survey was completed, which incorporated the external pathway connecting the various cave entrances and the cliff edges. During the period 2006–2010, further measurements and profiles were taken at base-stations and along the ceiling. A total of 207 different measurements have been recorded between the various topographic base-stations (including azimuth, elevation and distance). These topographic stations form a polygonal traverse of fixed primary stations, representing the centerline of the main cave galleries.

During the survey work, measurements were always recorded twice. If a significant difference was encountered, the measurement would be retaken a third time. A network of secondary base-stations was also established, usually radiating from most of the primary stations and reaching the contact of the ground surface with the cave walls. These were created to control the 'closing loop' errors in the survey polygons and to get an accurate areal plan of the galleries. The primary topographic stations were marked with 12 cm

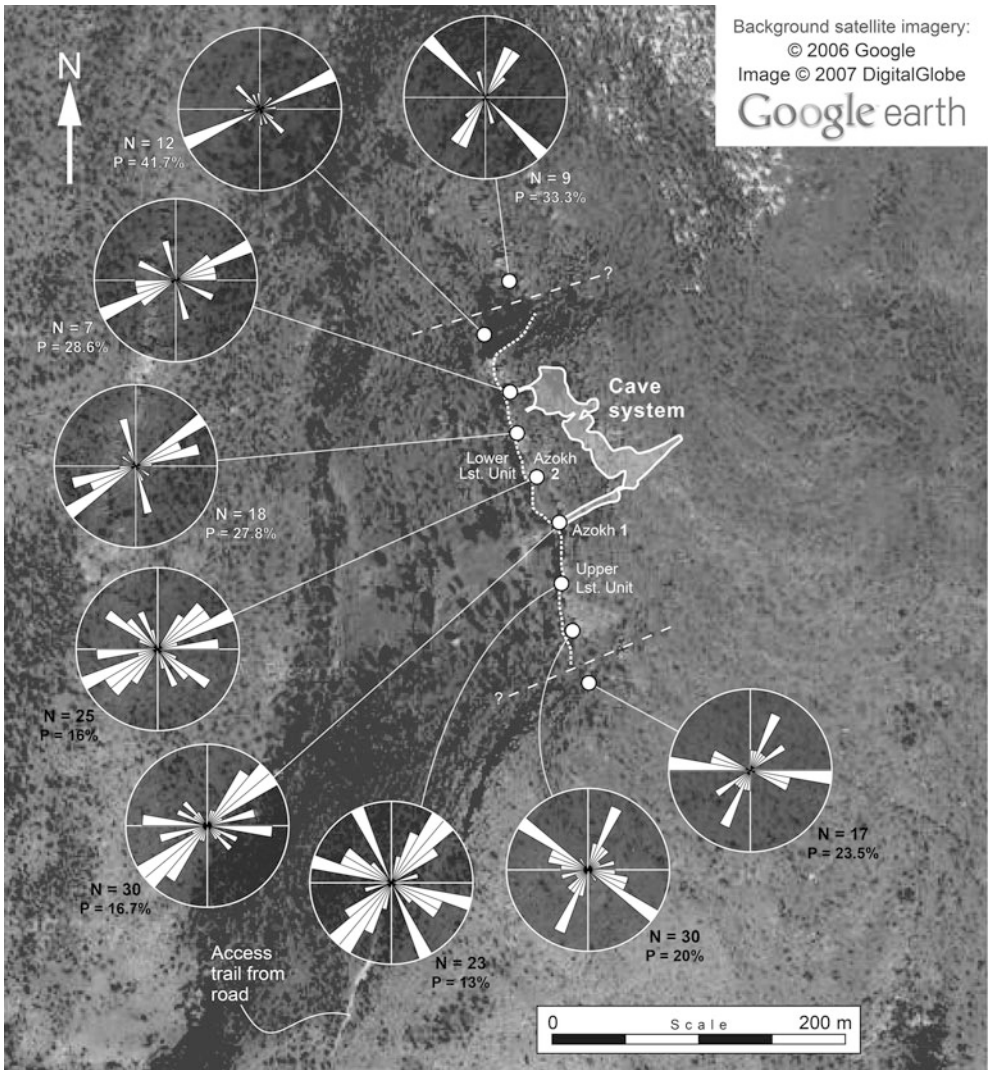

Fig. 3.7 Aerial view of the Azokh Cave area (sourced from Google Earth) with directional rose diagrams for sub-vertical joint sets developed in the limestone bedrock. Mapping was conducted along the central terrace of the escarpment (top of Lower Limestone Unit, base of Upper Limestone Unit) above the main entrance passages. Small filled white circles represent mapping locations on the terrace. Axes in rose diagrams represent geographic N–S and E–W, while each rose petal represents 10 degrees. N is the number of measurements per location, while P refers to the maximum perimeter value of each rose diagram, as a percentage of the total dataset. WSW to ENE trending dashed lines (with question marks) towards either end of the traverse intersect collapse features in the limestone bedrock and may be possible faults

nails and polyethylene labels on the ground and, where appropriate, discrete marker points on the limestone walls. In 2010, several transverse profiles were drawn using a minimum of 20 measurements per profile.

Computer analysis of the topographic data facilitated the creation of a 3-dimensional plot of the various base-stations (and survey lines connecting them) throughout the entire cave system. Speleological software used included *Therion* (Mudrák and Budaj 2010), *COMPASS Cave Survey Software* and *Visual Topo* (David 2008). The main 'centerline' of the cave system (running from Azokh 1 entrance around to Azokh 6) and the centerline of the external pathway (connecting these two particular entrances) produced a 305.57 m long polygon, with a 3-dimensional loop-closure error of 1.57% (>14 cm/station). However, the secondary base-station network created a mesh of triangles and loops (35 loops in total), which further corrected and controlled this closing error. As a result, the total 3-dimensional closing loop-error for the cave survey (with respect to the entrances) is only c. 0.61%. It is slightly lower again for the 2-dimensional plan (0.59%; in most cases >2 cm/station, and with a maximum of 14 cm over more than 2 km of total measurements). For the final assembly of the cave topography the closing loop-error was averaged to fit over the total length of measurements.

Results of the Topographic Survey

An accurate 2-dimensional plan of the presently accessible portion of the cave network at Azokh is presented in Fig. 3.8, based on the corrected plots of the various topographic stations described above. The accessible part of the cave is estimated to be about 1,840 m^2 in areal extent, although this is complicated by 3-dimensional considerations. An attempt has been made, for example, in Fig. 3.8 to provide an indication of the slope of the floor in the interior of the cave (see gray topographic contours in 1-m divisions). The sediment infill (floor level) is seen to rise towards the

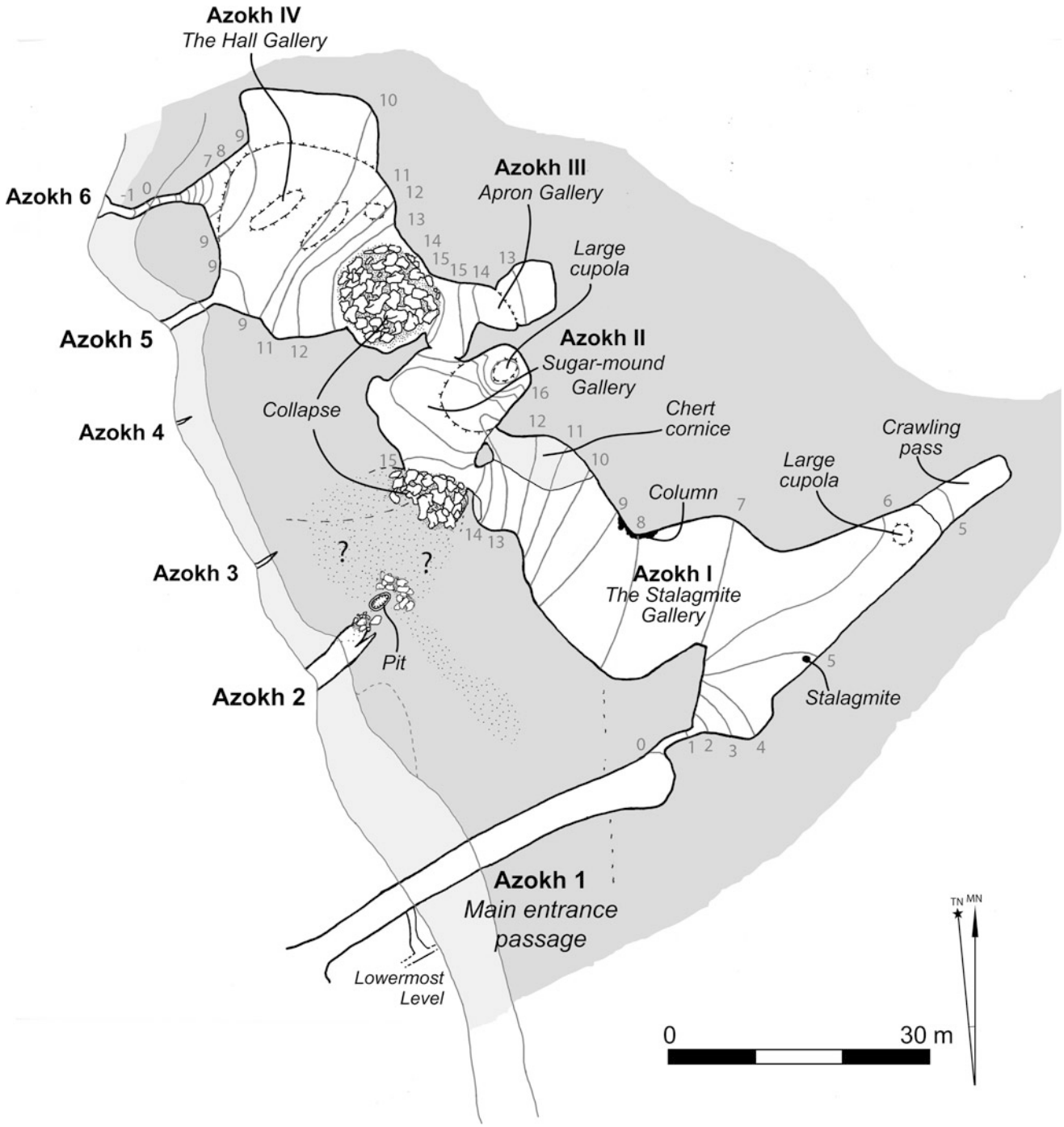

Fig. 3.8 Detailed plan map of Azokh Cave system. Entrance passages are denoted with Arabic numerals and internal chambers, or galleries, are differentiated with Roman numerals. Gray topographic contours (in meters) provide an approximate indication of the slope of the floor surface in the cave interior. The zero for these contours is the cave datum located in the rear of Azokh 1 passage

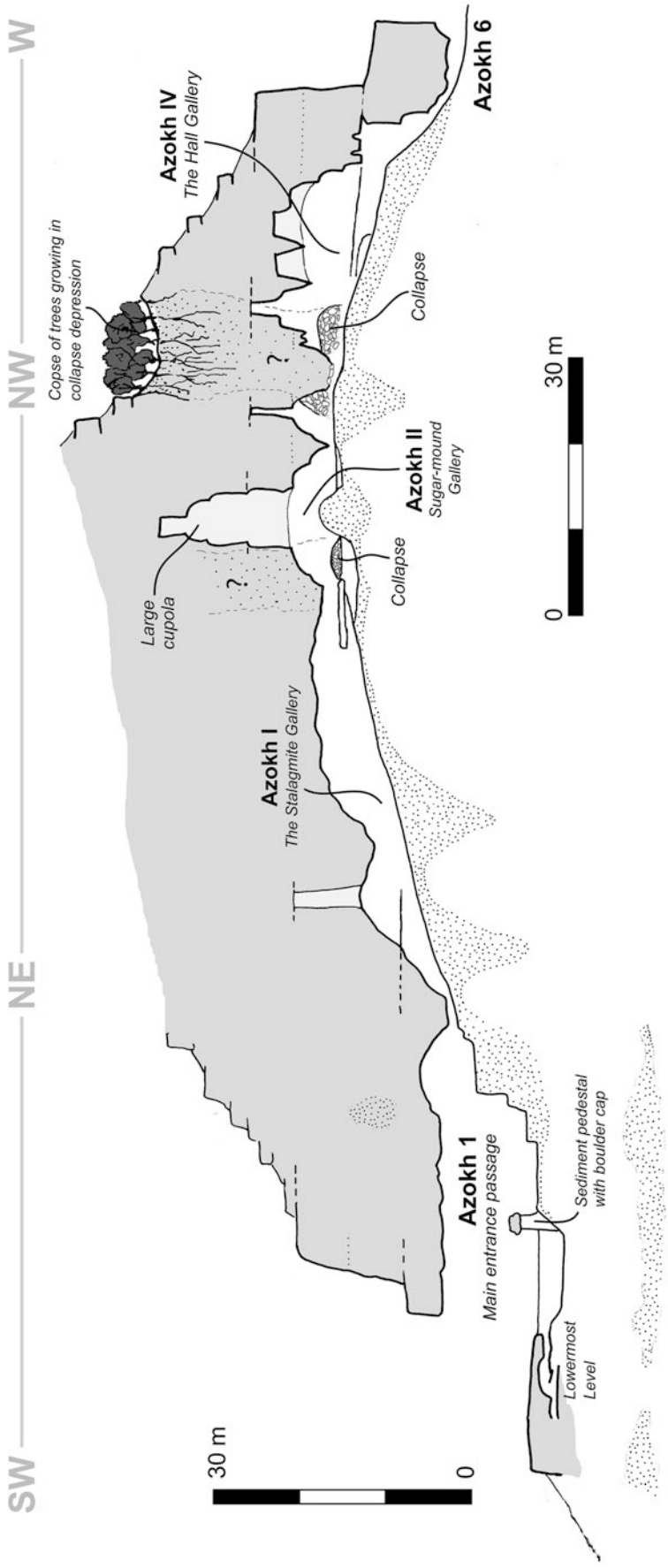

Fig. 3.9 Cross-section profile through the entire cave system at Azokh (entering through Azokh 1 passage and exiting through Azokh 6). The trajectory of the line of section is indicated across the top (note how it deflects around (bends) through approximately 180°). Horizontal and vertical scales are approximately equal

middle of the cave network. This elevation in the ground surface level is also quite apparent in the cross-sectional profile produced for the entire cave system (Fig. 3.9).

The cave system at Azokh is seen to comprise a series of broadly NW to SE trending chambers (Fig. 3.8). These are connected (to varying degrees) to the exterior by a series of orthogonally directed (i.e. NE to SW) entrance passages. The entrance passages are denoted with Arabic numerals (Azokh 1, 2 etc.) whilst the internal chambers are labeled with Roman numerals (Azokh I, II etc.). Six passageways have been identified to date, although only three of these (Azokh 1, 5 and 6) are sufficiently developed to permit access right the way through to the interior of the cave. Four separate internal chambers are identified (each with their own informal name, e.g., Azokh I – *The Stalagmite Gallery*). Murray et al. (2010) provided a simplified version of this map (their Fig. 3.2b) in which they identified five (I–V) internal chambers. This is rationalized to four here – specifically their chambers I and II have been amalgamated.

General Description of the Cave Galleries

Azokh 1: Main Entrance Passageway

The passageway labeled Azokh 1 is the main entranceway to the interior of the cave (Figs. 3.8 and 3.9) and it had been extensively excavated prior to the arrival of the current team (Huseinov 1985; Ljubin and Bosinski 1995; Lioubine 2002). Much of the present excavation effort has been concentrated in this passage since 2002 (Murray et al. 2010; Fernández-Jalvo et al. 2009, 2010). Azokh 1 runs for 35 m in a broadly straight NE/ENE direction from the entrance cornice. It is about 12–15 m high and 5–8 m wide and has a characteristic keyhole shape (Fig. 3.10). This represents what was once a rounded phreatic tube, which then followed a vadose regime forming a meander. The total floor area of this passage, from beneath the entrance cornice to the narrow passage at the rear, is 175–280 m^2. This narrow passage at the rear of Azokh 1 (Fig. 3.8; see also Fig. 3.10d) is less than 3 m long and it connects to Azokh I inner chamber.

Azokh 2, 3 and 4: Blind Passages

Azokh 2 is a short passage (it is only about 7.5 m long by 3.5 m wide) located NNW from Azokh 1 (Fig. 3.11; see also Fig. 3.8 for general location). A prominent NE-SW trending fracture (joint) in the bedrock runs the length of the roof and appears to have mediated the formation of the chamber. A large boulder collapse has blocked the rear of this passage and, on the exterior, a vertical pit occurs over this passage on the top surface of the *Upper Limestone Unit* (see relative positions of these features in Fig. 3.8). The boulder collapse prevents access to the inner galleries of the cave system and it has also limited the amount of archaeological excavation possible in the passage. Fernández-Jalvo et al. (2010) reported a partial skeleton dated to 1265 ± 23 years $C^{14}BP$ which was recovered near the top of the sedimentary sequence infilling in Azokh 2.

The locations of Azokh 3 and 4 are shown in Fig. 3.8 and the hillside panorama in Fig. 3.5a. Both are narrow and high, essentially widened joints with similar orientation trends to Azokh 1 and 2, and access to these is only possible for less than 1 m.

Azokh 5: A Recently Discovered Connection to the Inner Chambers

Access to the cave's interior through Azokh 5 was first discovered in 2004. This is a fairly short passage (only 10 m long) with a rounded roof, which continues inwards for 5 m before expanding upwards and outward and connecting to the Azokh IV chamber inside (Fig. 3.8). Large chert developments in the limestone feature prominently in the roof, and they are particularly conspicuous on the interior of the chamber. At the time of its initial discovery the gap between the sediment fill and the cave roof in Azokh 5 passage was only about 20 cm (Fig. 3.12). The ground surface was composed of unaltered, very dry loose sediment and the entrance to the chamber was hidden by vegetation.

Azokh 5 has proven to contain a relatively undisturbed sedimentary section replete with numerous fossils and archaeological artifacts. Fernández-Jalvo et al. (2010) reported modern human remains with associated charcoal [dated to ~2,300 years $C^{14}BP$] from near the top of the infill in the rear of this passage. The excavation work conducted in Azokh 5 since its initial discovery has improved access through this passage and, rather than crawling inside in a prone position, it is possible now to enter by walking and stooping.

Azokh 6: Vacas Passageway

This passageway is located at the northwestern extremity of the cave system (Fig. 3.8; see also Fig. 3.9) and it is the traditional exit route for local visitors to the cave. It takes its

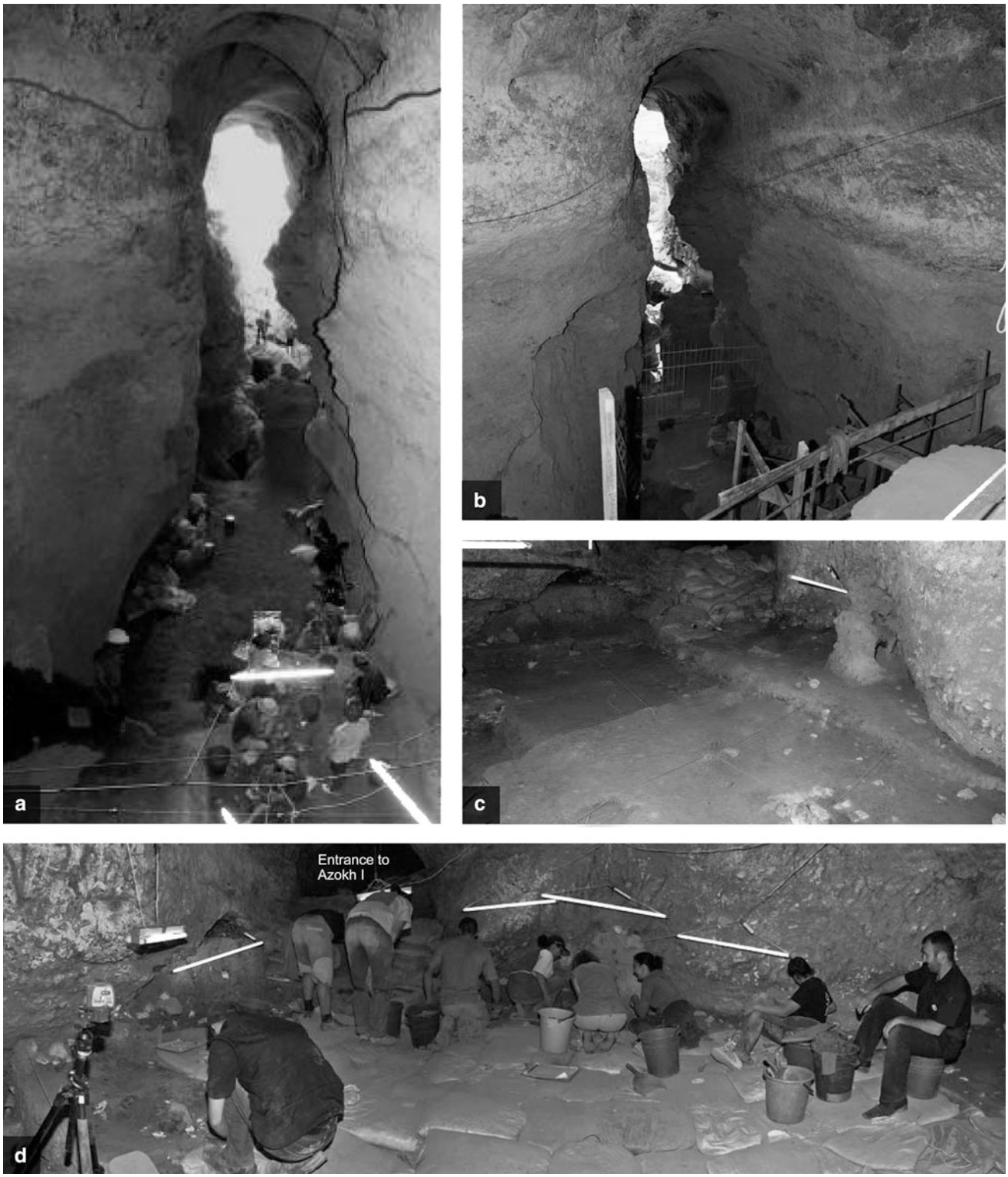

Fig. 3.10 Azokh 1, the main entrance gallery. **a**, **b** Photographs of the entrance passage taken from the top of the uppermost platform looking southwestwards towards the cave opening. The image in (**a**) is reproduced and slightly modified from Fernández-Jalvo et al. (2009). Note in (**b**) the scaffolding erected to support the section and the zip-line installed to assist in the evacuation of sacks of excavated sediment; **c**, **d** General views of the uppermost platform

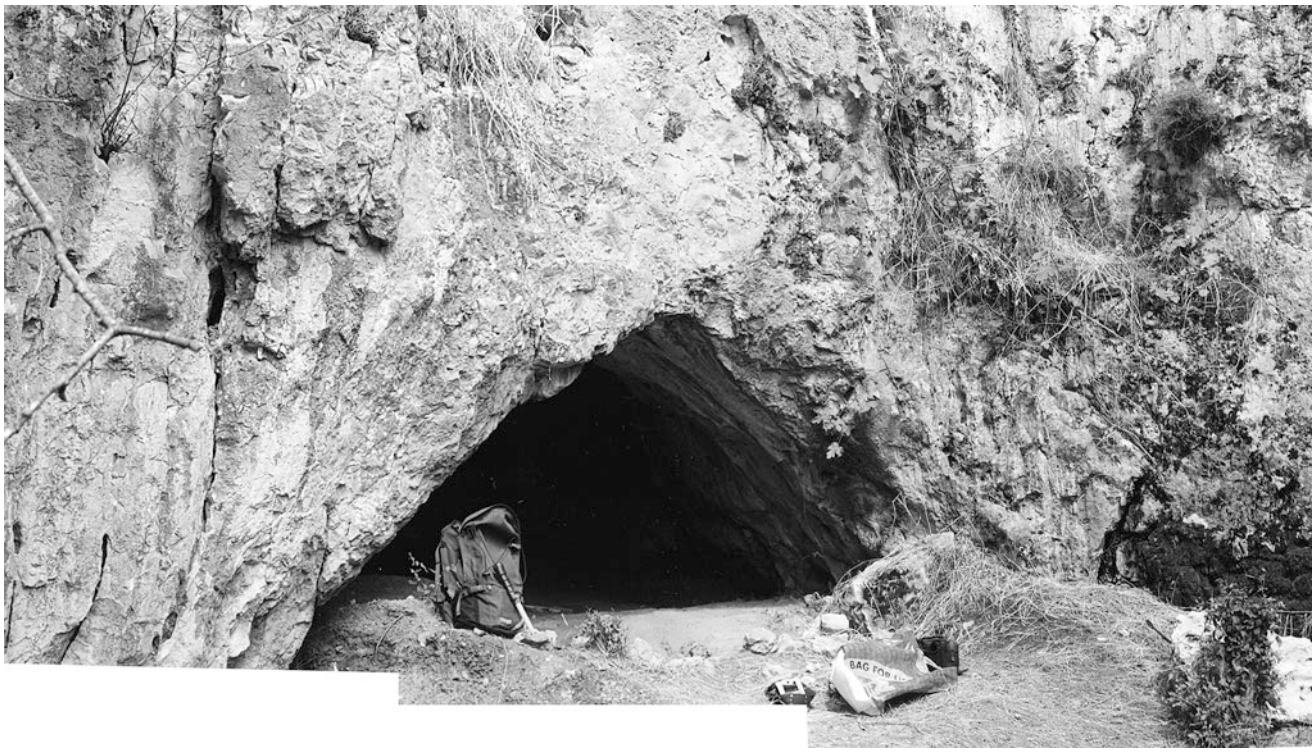

Fig. 3.11 Entrance to Azokh 2, photographed in 2004. Geology hammer and rucksack for scale

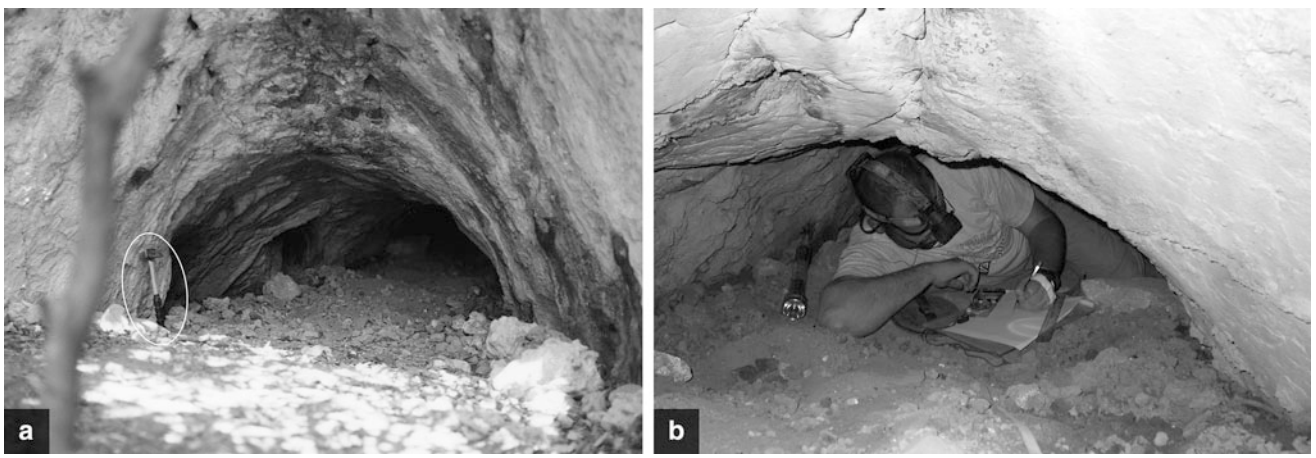

Fig. 3.12 Azokh 5 entrance. **a** Original (undisturbed) level of sediment fill in the passage just after the first survey was completed of the interior. Hammer (circled) for scale; **b** Early survey work being conducted through Azokh 5 passage, viewed from the interior

name from the Spanish word for cows – local livestock commonly frequent the entranceway and their dung may be thickly deposited underfoot. This narrow passage is about 12 m long (with a surface area of 7 m^2) and it rises upwards on entering the cave interior, before connecting with Azokh IV chamber inside.

Azokh I: The Stalagmite Gallery

With a total surface area of 843.5 m^2 the *Stalagmite Gallery* is the largest inner chamber of the cave system at Azokh (Figs. 3.13 and 3.14; see also Fig. 3.8 for general location). The name was originally coined by the previous excavation

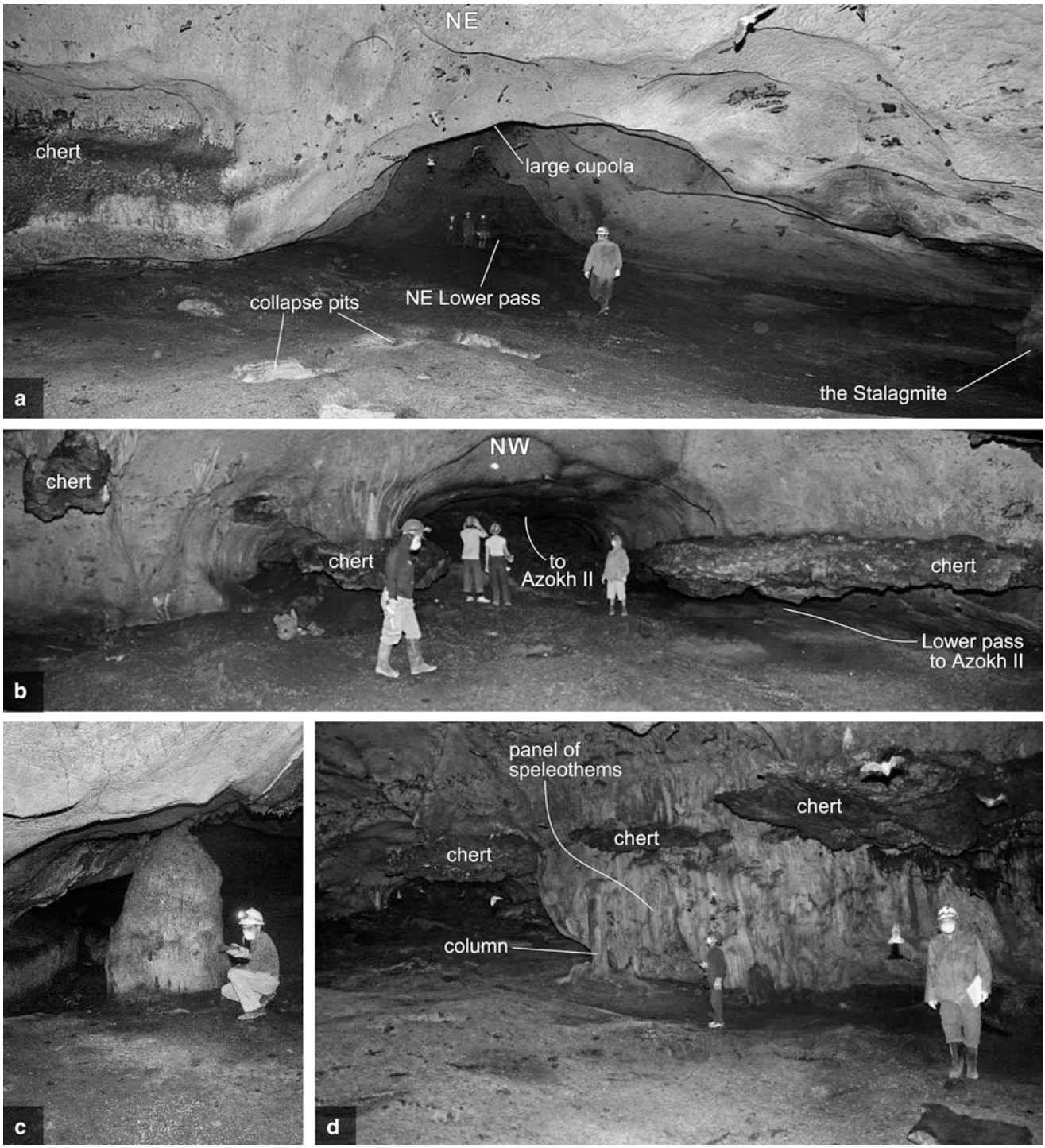

Fig. 3.13 Azokh I [*The Stalagmite Gallery*: Part 1]. **a** View of the NE branch of this gallery, as seen from the entrance passage. At the far end of the field of view are a lower pass and a high cupola. A large conspicuous stalagmite, which gives the gallery its name, is located at the extreme right of this image (along the SE wall of the chamber); **b** The termination of the NW branch of this gallery, leading into the second gallery (Azokh II). Note the thick bands of chert, which are laterally persistent for several meters, forming cornices; **c** The stalagmite; **d** The largest known panel of speleothems in the cave system, protected from corrosion by overlying chert cornices. This panel includes flags and a c. 2 m high column

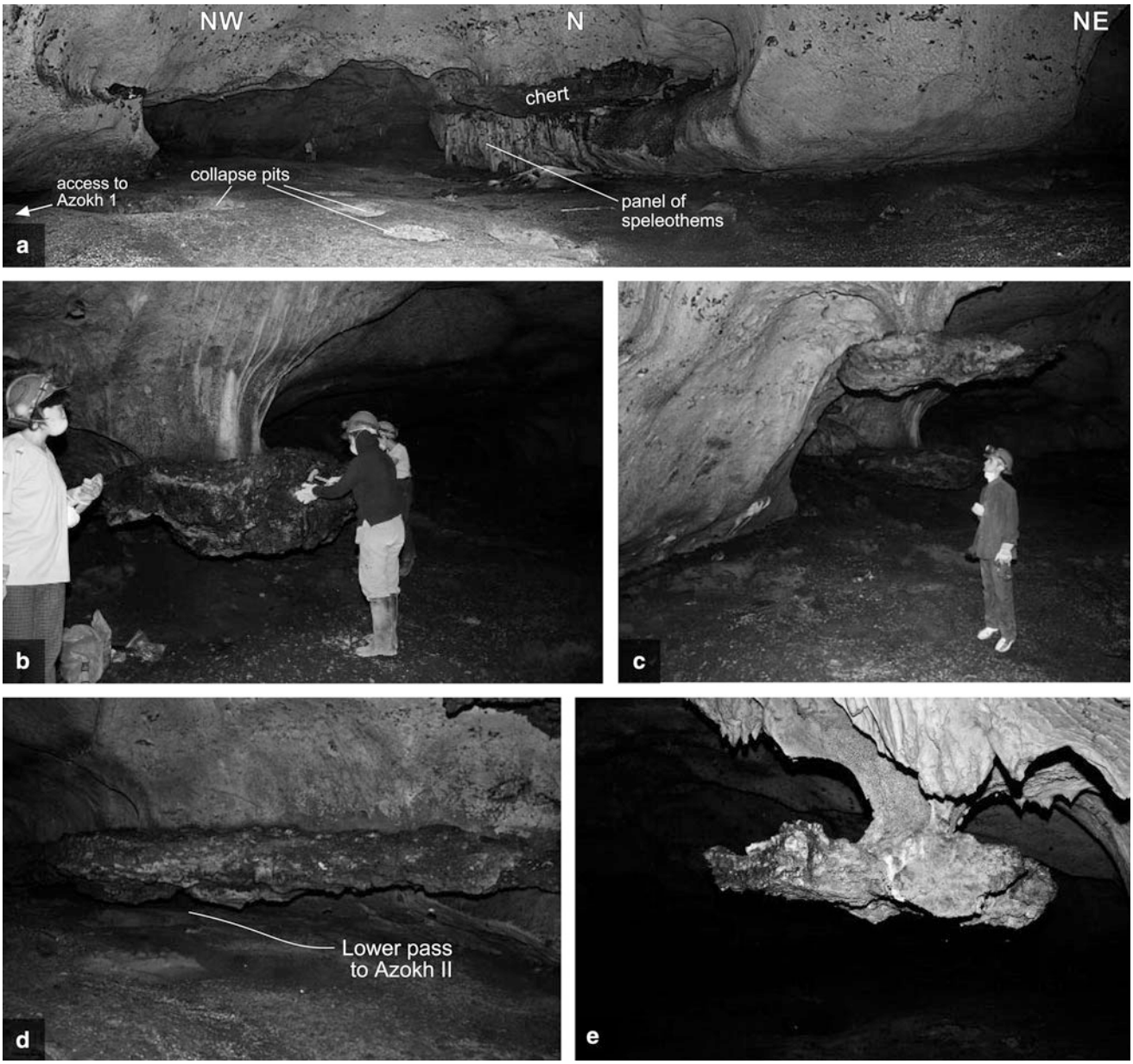

Fig. 3.14 Azokh I [*The Stalagmite Gallery*: Part 2]. **a** General panorama of the gallery from entrance passage from Azokh 1; **b–e** Detailed views of some hanging chert blocks, pendants and cornices. **b** Pedicled hanging block of chert; **c** View showing the spatial relationship of the hanging blocks in (**b**) and (**e**); **d** Large chert cornice with the lower pass to Azokh II: note the gentle slope of the ground surface; **e** Pedicled hanging block of chert. This structure is very narrow and the pendants in front of it (which are not stalactites) provide evidence of appreciable corrosion of the cave walls (probably by condensation-corrosion processes)

team (Huseinov 1985) in reference to the large conspicuous stalagmite found along the SE wall of the chamber (Fig. 3.13c), a short distance from the narrow connecting passage to Azokh 1.

The Azokh I chamber divides into two branches (Fig. 3.8), as follows:

- *Branch 1* continues internally from the rear of Azokh 1 passage in a NE direction, before terminating in a low cul-de-sac (Fig. 3.13a), at which point there is a distinctive inflection in the cave ceiling and the ground slopes slightly distally. This lower part of the gallery (overlain by the low ceiling) has a surface area of 38 m^2. The ground surface of the crawling pass is composed of loose sediment, most of which is completely undisturbed.
- *Branch 2* opens towards the left hand side (NW) as one enters from Azokh 1 passage and continues for some 47 m in a northwesterly direction (i.e. orthogonal to the first branch), before connecting with the next inner

chamber (Azokh II). There is a steady slope on the floor of this gallery, ascending 8 m elevation in less than 23 m. The NW end of this chamber ends with a large chert cornice on the northern wall (Fig. 3.13b). A second (lower-level) access route to Azokh II is present below this feature (Figs. 3.13b and 3.14d).

The limestone walls of the *Stalagmite Gallery* are mostly light in color, with broad and shallow concave surface depressions. In the northern wall of *Branch 2* a large band of overhanging chert is located at about 2.5 m above ground level. This is a common place for bats to congregate and, as a result, a half meter thick mound of guano has developed beneath it. This block of chert also protects parts of several speleothems covering the wall from corrosion. This panel of speleothems is about 3 m long and 2.5 m high, and stalactites, flags and a 2 m high column are present (Figs. 3.13d and 3.14a).

Very close to the walking passage connecting through to Azokh II, a large block of chert hangs from the ceiling via a narrow pedicle of limestone (Fig. 3.14e). This feature provides evidence for the intense corrosion of the cave walls during the late evolution of the karst system. A short distance beyond this (Fig. 3.14c), is another large block of chert hanging from the ceiling at waist level (Fig. 3.14b). It is less obvious, due in part to its close proximity to a large underlying debris cone of sediment (from a collapsed gallery).

The ground sediment in the Azokh I chamber is a sandy-clay, with a thin veneer of more clay-rich material. During the summer months, when excavation and survey work is in progress, this sediment is usually found to be slightly damp. The access route to Azokh II was dry during a visit made by PDA in November 2007. The ceiling in this part of the cave used to have a few thin straw stalactites, which were fairly recent in age and active during the summer. The debris of a large collapsed chamber is located nearby (Fig. 3.8) and possibly acts as a water reservoir for this feature. Several meter-scale depressions occur on the

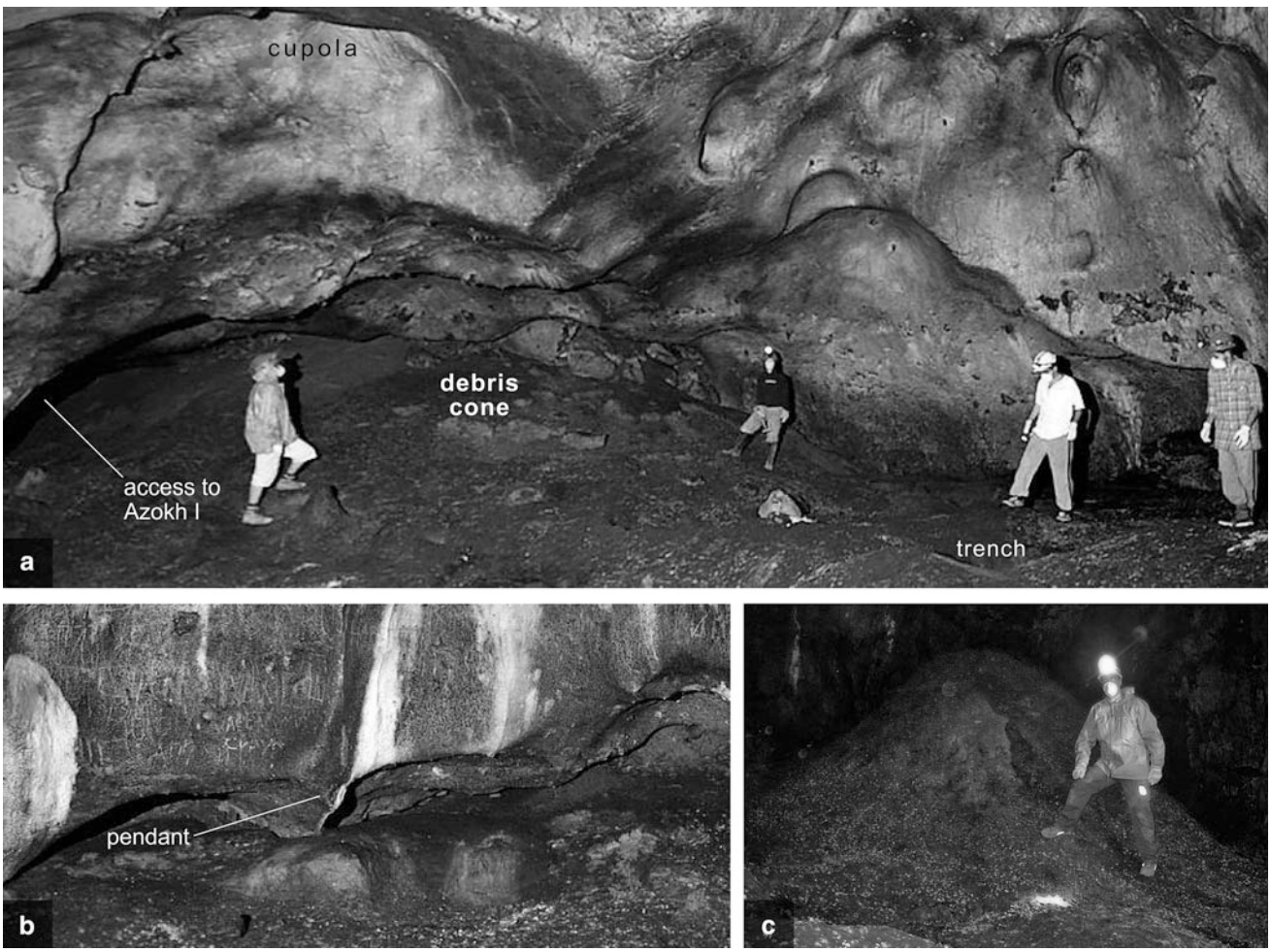

Fig. 3.15 Azokh II [*The Sugar-mound Gallery*]. **a** General panorama of the southwestern part of this cave gallery. A boulder choke and resultant debris cone blocks access to it from the upper pit over Azokh 2 on the exterior (see Fig. 3.8). **b** The NW wall of the gallery, composed largely of pendants; **c** Very large pile of bat guano present inside the chamber. The gallery is named after this feature

ground in this chamber and are labeled as 'collapse pits' in Figs. 3.13a and 3.14a; however, it is equally quite plausible that they were excavated by local visitors to the cave.

Azokh II: The Sugar-Mound Gallery

The *Sugar-Mound Gallery* is broadly oval-shaped with a surface area of 178 m^2 (Fig. 3.15). A conspicuous characteristic of this chamber is a very large pile of sediment with a rounded profile, which is covered by a very substantial amount of guano (Fig. 3.15c) and which gives the name to this chamber. It is located close to the northeastern wall, beneath a large cupola indicated on the cross section in Fig. 3.9. The walls of the chamber are noticeably darker compared with Azokh I and are covered with a brownish cinnamon-like color coating.

Upon entering the *Sugar-Mound Gallery* (Azokh II) from Azokh I, just to the left by the western wall is a significant collapse feature with decimeter-scale boulders of limestone (labeled "debris cone" in Fig. 3.15a). The deposit is largely clast-supported and finer reddish-brown sediment makes up the matrix in the interstitial areas between the boulders. This feature forms a sediment cone which extends NW across the Azokh II chamber and also SE into the (NW) terminal portion of Azokh I (*Branch 2*). Despite the scale of this collapse, no clear sign of it is evident on the exterior of the cave. We suggest that this allochthonous sediment cone possibly corresponds to a collapse dome which remained largely internal, within the *Upper Limestone Unit*, and which probably has kept an air cavity above it.

Azokh III: The Apron Gallery

This inner chamber is developed on two topographic levels and has a total surface area of 93 m^2 (Fig. 3.16). Entrance to this gallery is made from Azokh II through a low crawl-way (Fig. 3.16a), which leads directly onto the upper of the two levels. A fairly steep incline on the ground surface leads down in an easterly direction towards the lower level of the chamber (Fig. 3.16d). This slope is principally due to the presence of an apron of debris radiating from a very large collapse feature (Fig. 3.8).

The walls of the *Apron Gallery* have experienced intense weathering, possibly due to the concentrated presence of bats there. Signs of micro-corrosion are clearly evident on many surfaces:

- Shallow concave (millimeter-scale) cavities, probably formed by chemical corrosion of the limestone *and*
- Striations (cuttings) most probably formed by continuous erosion from the claws of bats.

The exit from this particular chamber through to Azokh IV is positioned on the same topographic level as the entrance (it is a horizontal narrow path made by the footsteps of frequent visitors), and the connection is a short, narrow passage, which skirts around the periphery of the large debris cone.

Azokh IV: The Hall Gallery

This large gallery has a broadly rounded or ovoid shape in plan and occupies a total surface area of 442 m^2 (Fig. 3.17; see also Fig. 3.8). At the northern end of this large and spacious chamber, a large chert cornice protects and supports the roof of a small, but quite distinct, underlying side-chamber or "hall" (Fig. 3.17a).

A large collapse feature, filled with large limestone boulders, with finer sediment infilling the interstitial gaps, is located at the SE end of the *Hall Gallery* (labeled "debris cone" on Fig. 3.17d). This allochthonous deposit is a continuation of the boulder cone forming the NW wall of the *Apron Gallery* (Azokh III), discussed previously. On the hillside outside the cave, positioned broadly above this feature, there is a dense copse of trees growing in the depression (doline) created by this collapse (Fig. 3.5a, c; see also the cross section in Fig. 3.9). These trees sink their roots some 20 m vertically through the soil and the roots themselves are visible in the cave chamber beneath.

The exit from the *Hall Gallery* (Azokh IV) to the exterior may be made through either Azokh 5 or Azokh 6 passages on the western side of the chamber (Fig. 3.17c). The latter involves a moderately steep descent down a sloping surface and through a narrow pathway corridor, which then leads to the outside of the cave (see Fig. 3.9).

Geophysical Investigation of the Cave System

The topographic mapping of the cave system at Azokh, discussed above, and illustrated in Figs. 3.8 and 3.9, can only ever provide an indication of the open spaces that are possible to physically explore and document. The full extent of the various karstic conduits is obscured by the level of sediment infilling them and, in some cases (such as Azokh 2), blocking of the galleries by collapse features. Geophysics provides a tool to investigate the nature of the subsurface within the cave. DC electrical resistivity has proven a useful method for constraining the boundary between buried limestone bedrock and overlying unconsolidated sediments

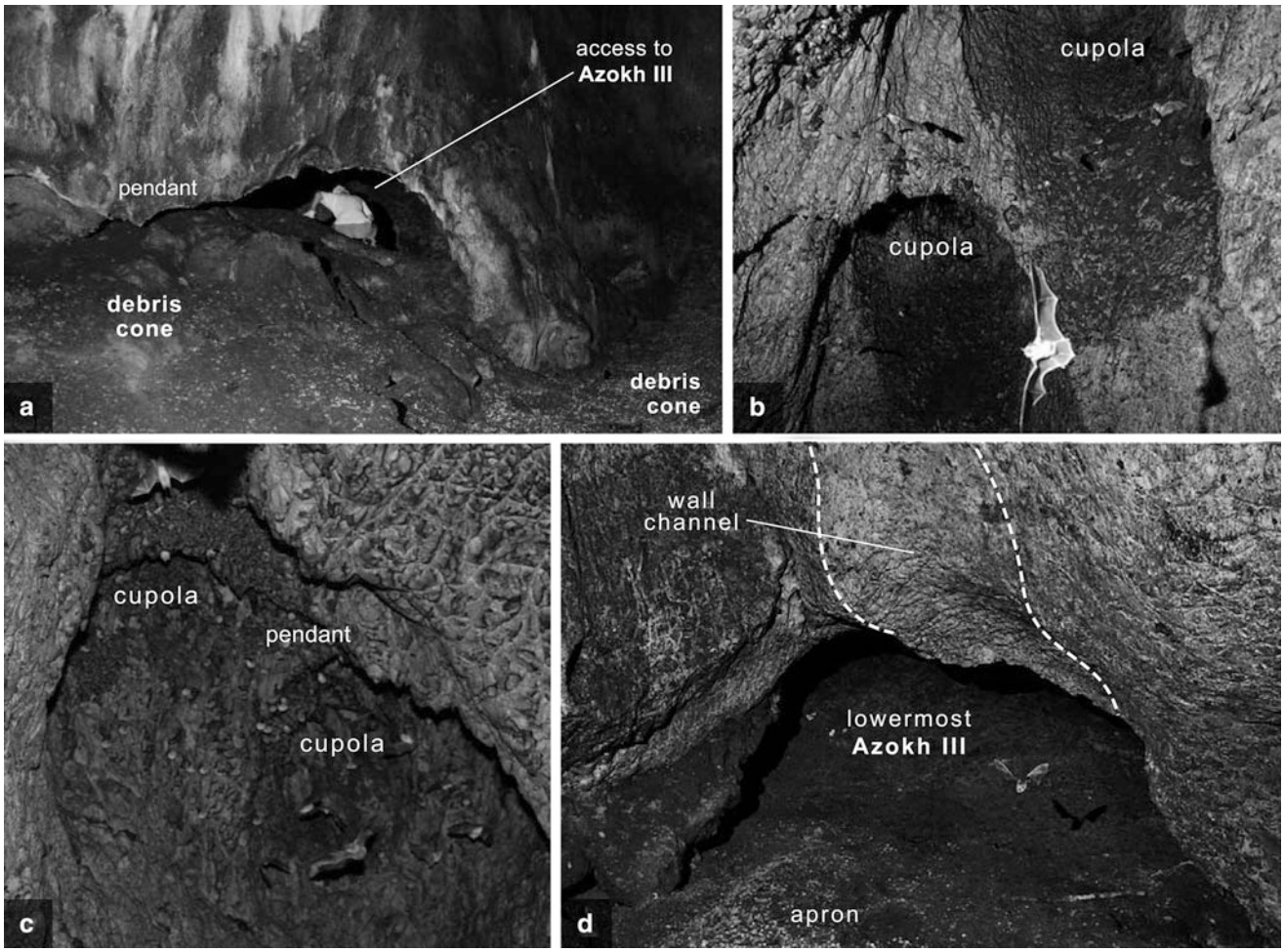

Fig. 3.16 Azokh III [*The Apron Gallery*]. **a** Access route to this gallery (from Azokh II); **b**, **c** Complex cupolas in the ceiling of Azokh III. Note the coarse texture of the walls and the darkening because of the activity of bats; **d** View of the topographically lowermost part of this gallery from the general cave pathway. Note the possible carved 'channel' feature in wall

(e.g., Aracil et al. 2003; Porres 2003). The application of this particular technique makes it possible to estimate infill thicknesses and the volume of sedimentary material sitting on the rocky floor of the cave; to determine the sectors of the cave system with the greatest accumulation of infill; to characterize the different types of infill; and, as far as possible, identify possible cavities in the limestone bedrock beneath the sediments (e.g., Gautam et al. 2000; Griffiths and Barker 1993; Zhou et al. 2000).

Materials and Methods of the Geophysical Survey

As a complementary study to the physical description of the Azokh Cave system, a geophysical survey was conducted both internally and externally (Fig. 3.18). The survey lines were concentrated near the various entrances and across the top surface of the limestone escarpment (*Upper Limestone Unit*; see Fig. 3.5a), with the dual purpose of identifying new subsoil cavities and determining the extent of fracture development and its relationship to cave formation.

Electrical resistivity tomography is a geo-electrical surveying method that analyzes subsoil materials according to their electrical impedance, which, in other words, allows them to be differentiated according to their resistivity (Aracil et al. 2002, 2003). The level of concentration of ions which carry the electrical signal depends on the nature and composition of the rocks and sediment and also the degree to which they are compacted or porous, which in turn influences their fluid content. Greater mobility of ions results in greater electrical conductivity or conversely less resistivity. This parameter produces 2-dimensional or 3-dimensional profiles which allow the materials at different depths to be investigated at different degrees of resolution (e.g., Martínez-Pagán et al. 2005).

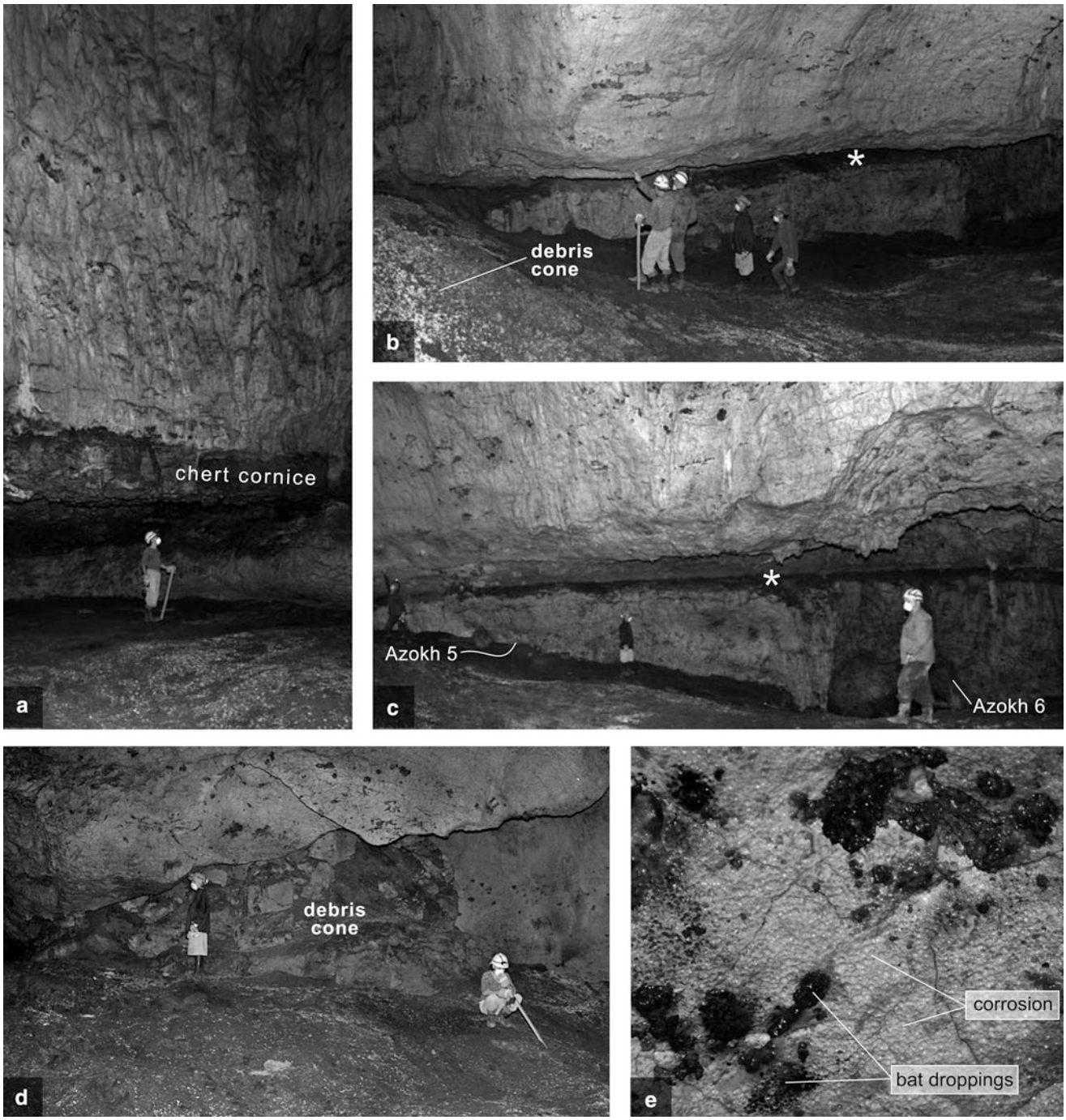

Fig. 3.17 Azokh IV [*The Hall Gallery*]. **a** Small side-chamber in this gallery, protected by an overlying layer of chert. Note the corrosion evident on the walls; **b**, **c** General views of the western side of the *Hall Gallery* showing the inclined surface of the sediment apron from the collapsed doline. A major bedding plane interface between the *Upper* and *Lower Limestone* units is indicated with a white asterisk in both photographs. The exits to the exterior through Azokh 5 and 6 passages are also indicated in (**c**); **d** View of the boulder choke (debris cone) feature (looking east across this gallery); **e** Detailed view of corrosion on the limestone walls of the gallery. This picture is about 6 cm wide

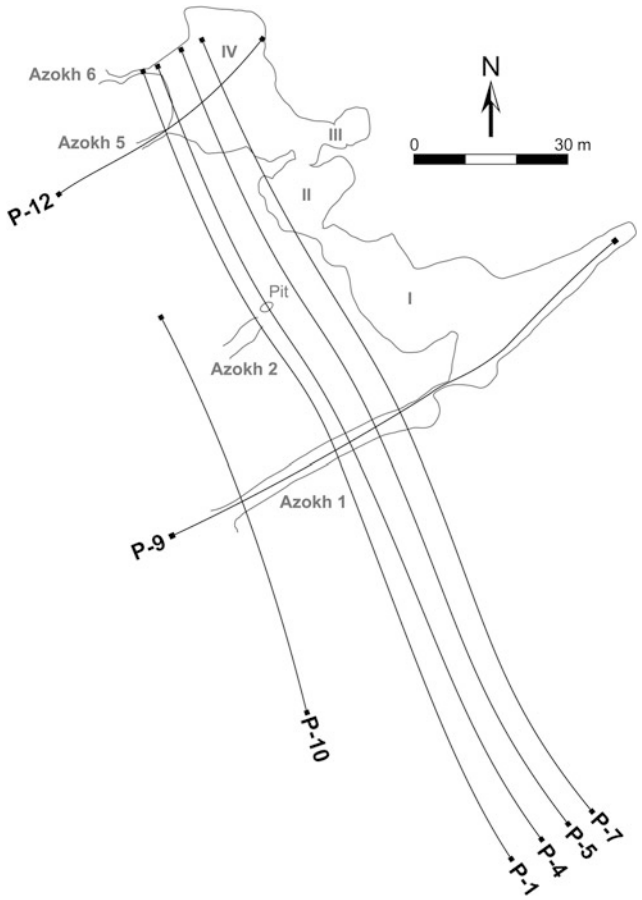

Fig. 3.18 Location (plan) map for geophysical electrical resistivity survey lines presented in Figs. 3.19, 3.20 and 3.22 and discussed in the main text. An outline of the cave system at Azokh is shown for ease of reference (internal chambers are denoted with Roman numerals). Lines P-9 and P-12 were taken from the interior of the cave, out through entrance passages (Azokh 1 and 5 respectively) and down the exterior hillside. Line P-10 was taken on the exterior of the cave, at the level of the entrance walkway to Azokh 1. Lines P-1, P-4, P-5 and P-7 were also taken externally, but at a higher topographic level, on the top surface of the limestone escarpment (*Upper Limestone Unit*) on the hillside

The resistivity in the rock or sediment will depend fundamentally on four factors:

1. The proportion of pore volume within the context of the total volume of the rock. Lower resistivity may be expected where there is a greater volume of pores (high porosity), provided these are filled with water, clay, etc.
2. The geometric layout of the pores (known as the formation factor). Limited pore morphology or a disconnected pore layout will lead to greater resistivity.
3. The nature of the material infilling the pores. If empty (vadose) cavity spaces are present, resistivity should be abnormally high, given the dielectric properties of air. Conversely, the greater the proportion of water-filled pores, the lower the resistivity, as the electric current circulates more freely through water than it does through air.
4. The resistivity or conductivity of the pore water concerned. Saline water, for example, has higher conductivity than fresh water. This will have the effect of altering the resistivity of the rock or sediment in which it is found (e.g., Sumanovac and Weisser 2001).

The electrical resistivity readings were recorded at Azokh Cave using a multi-electrode array set out along a set linear distance (see Fig. 3.18). The electrodes were pushed into the sediment by hand; however, where the ground surface was particularly rocky, a hammer was utilized. The degree to which the electrical current penetrates the subsurface is dependent on the electrode spacing – the wider the spacing, the deeper the penetration. In order to generate useful plots of the acquired geophysical data, it is necessary to link and correct the various survey lines to the cave topography (discussed above), to compensate for differences in slope.

Results of the Geophysical Survey

The results from the geophysical survey are presented in Figs. 3.19, 3.20, 3.21 and 3.22. Figures 3.19, 3.20 and 3.22 show vertical sections through the substratum which are color-coded according to their differing electrical resistivity properties (see legend at the bottom of each profile). In all of these profiles, it is possible to differentiate the subsoil from the limestone bedrock with a fair degree of clarity, due to the highly pronounced geo-electric contrast between both units. The unit comprising the sediment infill is more conductive or, conversely, is not very resistive; whereas the unit that forms the rocky substrate is very resistive, which is to say that it transmits the electric current with great difficulty, giving high resistivity values as a consequence.

Two electrical resistivity profiles from Azokh 1 passage (P-9), and the surrounding area outside (P-10), are shown in Fig. 3.19. Section P-9 is 175 m in length and runs from the interior of the cave (Azokh I: *The Stalagmite Gallery*), out in a broadly SW direction through Azokh 1 and down the hillside outside. This section shows the extent of the limestone bedrock as areas of relatively high resistivity directly beneath the floor of Azokh 1. This is the main area of excavation at present and the presence of bedrock in this part of the cave had been confirmed during previous geological and sedimentological survey work (see the cross section of this passage provided by Murray et al. 2010, their Fig. 3). Electrical resistivity profile P-9 (Fig. 3.19a) provides a more complete impression of the full extent of the limestone bedrock and, more significantly, suggests that there may be several infilled cavities beneath the present floor level; that is

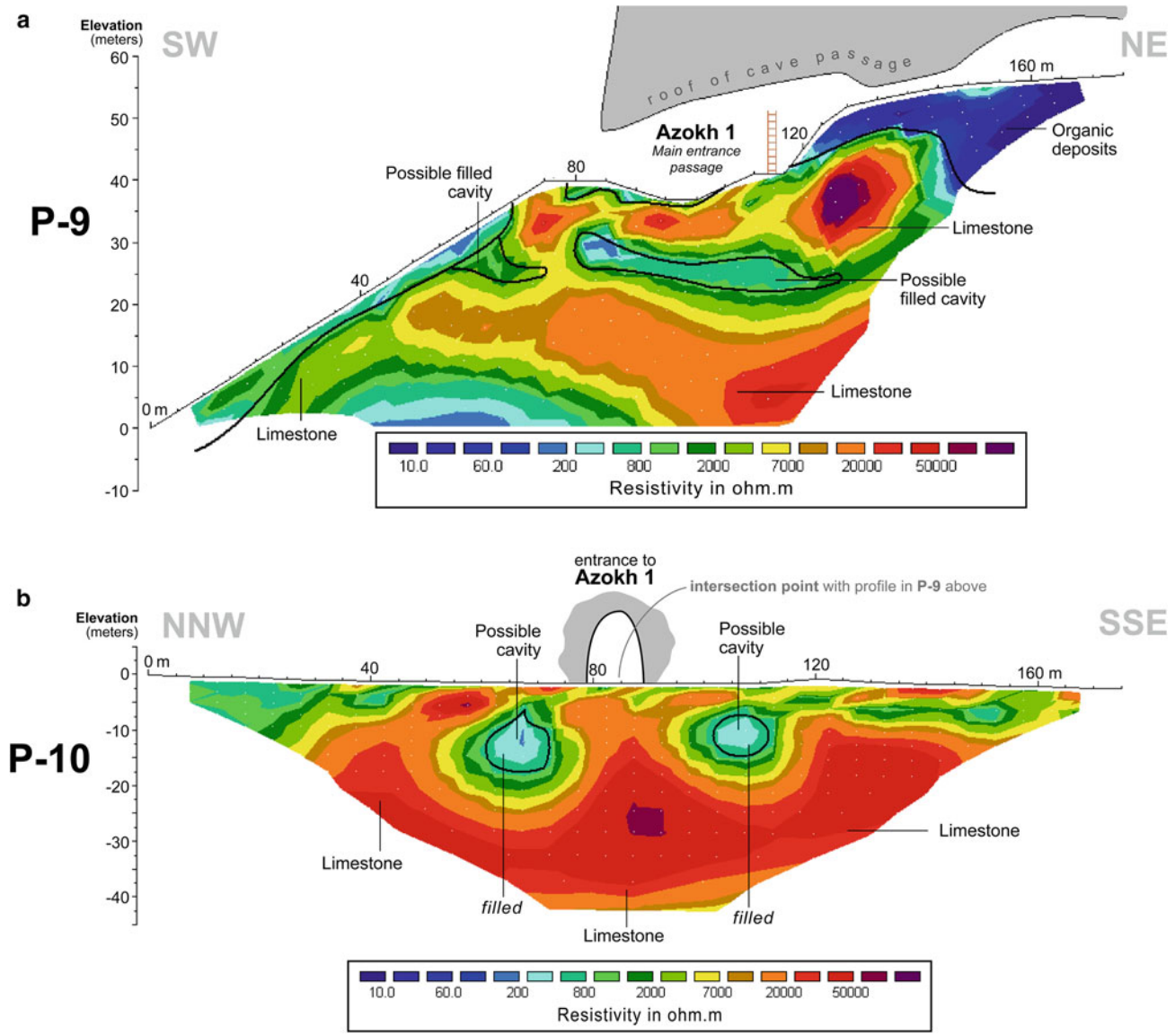

Fig. 3.19 2-D electrical resistivity profiles from Azokh 1. The two profiles intersect outside the cave at the mouth of the passage (see Fig. 3.18 for general location). **a** Profile P-9 was measured along the long axis of Azokh 1, in a SW (external) to NE (internal) direction, and shows the presence of a possible infilled chamber at about 8–10 m depth beneath the cave floor; **b** Transverse profile P-10 [broadly perpendicular to P-9] showing two possible infilled cavities at around 5–8 m depth beneath the surface. The cavity on the left may possibly correspond to the SW side of the cavity identified in P-9

lower levels not yet reached or investigated within the cave system. Resistivity profile P-10 (Fig. 3.19b) was measured across the entranceway to Azokh 1 passage in a NNW to SSE direction, broadly orthogonal to profile P-9. The intersection between these two profiles was at the cave mouth and is indicated on Fig. 3.19b (see also Fig. 3.18). This transverse section also suggests the possible presence of two discrete filled cavities at a lower level in the cave system.

Electrical resistivity profile P-12 was taken from Azokh IV (*The Hall Gallery*) and out through Azokh 5 passage (Fig. 3.20; see also Fig. 3.18 for general location). Importantly, this section indicates at least 10 m vertical thickness of sediment infilling the inner chamber. Excavation work is at a very early stage in this relatively undisturbed part of the cave and these geophysical results suggest considerable potential for future archaeological investigation there.

A number of additional 2-dimensional electrical resistivity profiles were recorded through the interior of the cave system and, in all, a clear differentiation between solid limestone bedrock and overlying unconsolidated sediment was observed. This facilitated the measurement of infill thickness from all the resultant sections, which then provided data for a points file with all the thicknesses recorded.

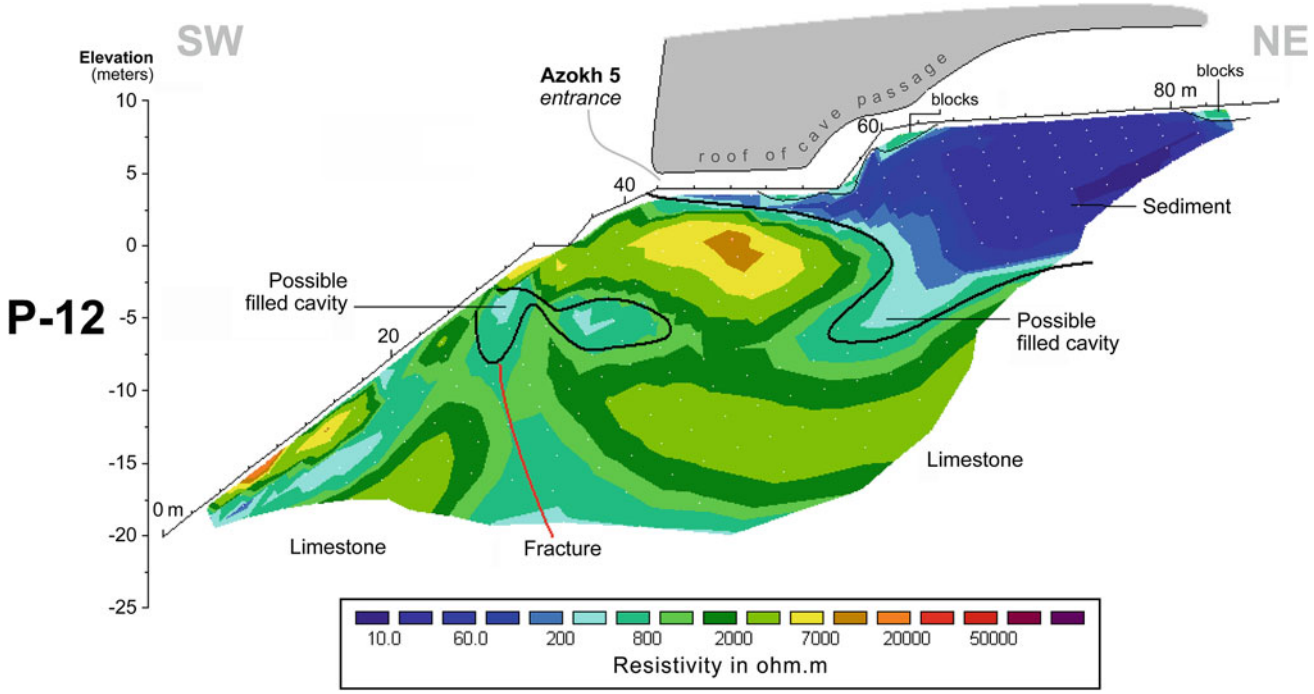

Fig. 3.20 2-D electrical resistivity profile P-12 through Azokh 5 passage. The large area of low resistivity (upper right on the profile) suggests appreciable sediment thickness in the inner chamber at that location. See Fig. 3.18 for general location of profile

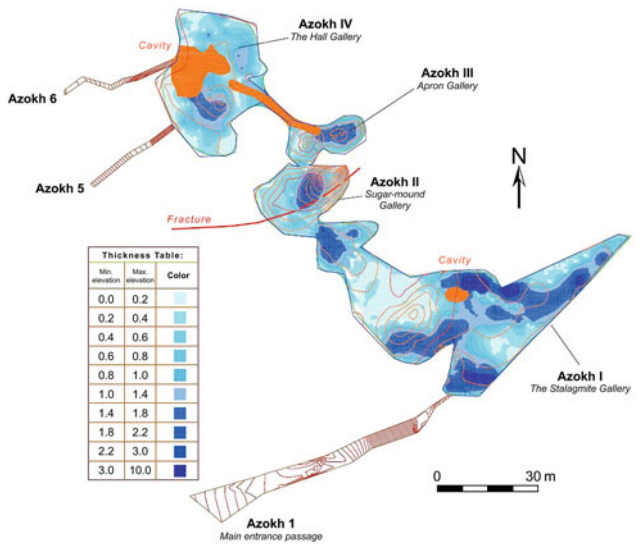

Fig. 3.21 Isopach plan map of entire sedimentary infill of the inner cave system at Azokh, calculated from electrical resistivity profiles

Using these values an isopach map of sediment infill thickness was generated (Fig. 3.21). According to this map, a concentration of thicker amounts of infill are observed in Azokh I (*The Stalagmite Gallery*), principally at the SE end, where it reaches thicknesses of between 2 and 3 m at various points and where areas with infill thicknesses of between 1 and 2 m are also frequently encountered.

Other areas of the interior of the cave also have elevated thicknesses of cave fill (Fig. 3.21) such as:

1. The area close to the entrance to Azokh II (*The Sugar-mound Gallery*) – probably related to the large cone of collapsed sediment;
2. The central area of Azokh II (*The Sugar-mound Gallery*) – probably related to the large pile of sediment and guano located there (see Fig. 3.9);
3. The lower level within Azokh III (*The Apron Gallery*); and
4. The south central portions of Azokh IV (*The Hall Gallery*).

Although the isopach map in Fig. 3.21 was drawn with all the infill considered as a homogenous entity, it is quite likely that the sediments do not all share a common origin. Beneath the organic surface layer of bat guano, which is in itself highly variable in thickness, part of the infill could be the product of the accumulation of coarse, medium and fine sediment detritus, including from the dissolution and fragmentation of limestone that forms the bedrock of the hillside.

The morphology and layout of the various cave galleries was probably strongly influenced by the presence of fractures in the limestone (Figs. 3.6 and 3.7), which would have logically been the conduits through which water flow was focused. An effort was made to analyze these fractures using electrical resistivity. Several parallel profiles (P-1, P-4, P-5 and P-7) were measured on the external surface of the

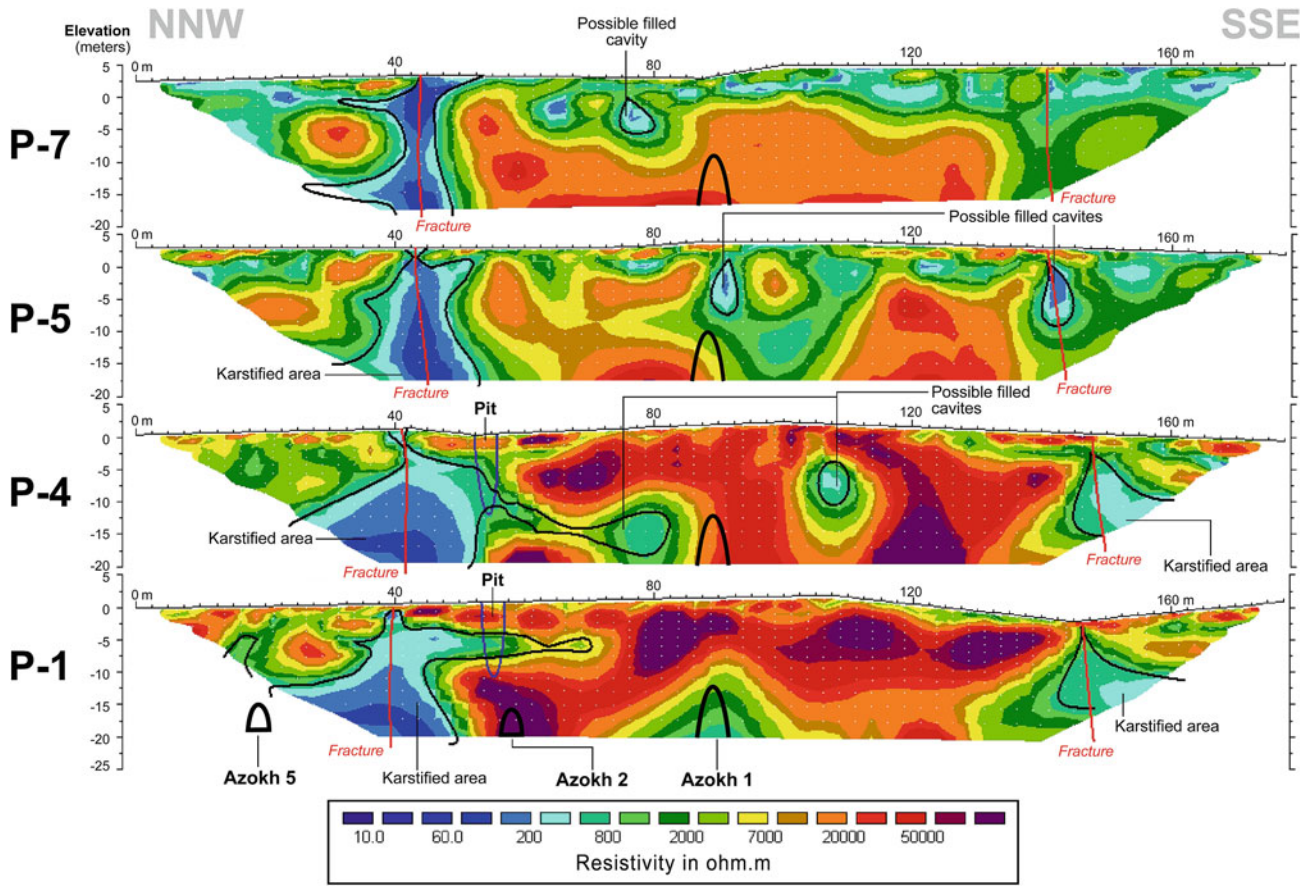

Fig. 3.22 Parallel 2-D electrical resistivity profiles (P-1, P-4, P-5 and P-7) taken sequentially across the top of the *Upper Limestone Unit* hosting the Azokh Cave system. See Fig. 3.18 for location details and also Fig. 3.5a for a general panoramic view of the hillside

limestone escarpment (Fig. 3.22; see Fig. 3.18 for general location), specifically on the top of the *Upper Limestone Unit* (see Fig. 3.5a). These profiles identify certain anomalies, which, due to their morphology, must represent fractures in the limestone, in which the circulation of water, and deposition of finer sediment, results in them displaying low resistivity values.

The anomalies interpreted as fractures and possible cavities are indicated in Fig. 3.22. A large conductive anomaly is evident towards the start (towards NNW) of each of the profiles, at about the 40–45 m point, and this may relate to a large fracture that runs through Azokh II gallery. The importance of this anomaly is that it corresponds to the inner chamber with the highest ceiling (cupola) within the cave system (see section in Fig. 3.9).

The profiles taken from the external surface of the hill in Fig. 3.22 also showed several fractures and possible cavities, apparently unconnected with the presently accessible part of the cave system. Some of these appear have an exit on the upper part of the *Upper Limestone Unit* through a shaft visible on the surface on the hillside (see Figs. 3.8 and 3.18 for location of this "pit" feature; it is also labeled on profiles P-1 and P-4 in Fig. 3.22).

Discussion

The plan of the cave system at Azokh presented in Fig. 3.8 is the most detailed and accurate version produced to date. The structural geological data in Fig. 3.7 shows that strongly

developed conjugate NE to SW and NW to SE joint sets are present in the limestone bedrock across the cave system, and these have influenced the orientation of the Azokh cave chambers beneath in the subsurface beneath (compare to Fig. 3.8). Sub-vertical joints appear to deflect away from this preferential cave system orientation at the northern and southern ends of the joint traverse. These data, combined with an interpretation of the aerial photograph presented in Fig. 3.7, along with the landscape panoramic in Fig. 3.5a, suggest the possibility that the thick limestone escarpment hosting the cave system may be bounded to the north and south by two large collapse features (*perhaps* influenced by the possible presence of two ENE-trending, sub-parallel faults; see Fig. 3.7).

The geophysical (electrical resistivity) survey work has shown a system of hidden galleries beneath Azokh 1 (Fig. 3.19). Recent clearing and excavation work in the basal entrance trench of this particular cave passage has revealed a small gallery, which is not infilled by sediment (Fig. 3.23; its position is also indicated as "*Lowermost Level*" in Figs. 3.8 and 3.9). This lowermost known level within the cave system was completely undisturbed when first discovered and contains several speleothems, including a spectacular "Christmas tree" shaped dogtooth calcite deposit (Fig. 3.23a–d). The latter grew subaqueously and indicates that the chamber was at least partially submerged, at least to the top level of the "tree". A speleothem development covered the entrance to this lower chamber (Fig. 3.23e, g).

At present, Azokh Cave does not follow a path for major conduits receiving groundwater recharge from higher levels in the limestone above, or indeed from the surface. On the contrary, it presents a 3-dimensional structure of large oblong-contour galleries directly connected laterally (Fig. 3.8). The keyhole profile of Azokh 1 passage (see Fig. 3.10a, b) suggests transition from phreatic to vadose conditions and is an indication of an epigenic cave system. According to Klimchouk (2007, 2009) in epigenic speleogenesis the process is dominated by shallow groundwater systems receiving recharge directly from above or areas immediately adjacent. The development of different levels or "storeys" at different elevations within the cave system thus reflects a progressive lowering of the water-table due to the evolution and incision of river valleys in the surrounding region. Thus upper storeys are older than lower ones. However, the presence of numerous cupolas (see discussion below; Fig. 3.24); pendants of isolated rock structures suspended from the cave ceiling (essentially the remains of rock pillars separating karstic channels cut through closely spaced paragenetic ceiling channels; for example see Fig. 3.14b, c, e); and abundant signs of dissolution or corrosion on the walls of the cave seems to suggest a hypogenic mode of speleogenesis. If *both* epigenic *and* hypogenic interpretations are valid, it may possibly suggest a polygenic origin for the formation of the cave.

Cupolas are dome-shaped solution cavities or wide vertical chimneys, which terminate abruptly and develop in certain cave ceilings. They are thought to form by condensation corrosion by convecting/circulating air (Osborne 2004; Piccini et al. 2007). According to Osborne (2004), cupolas are common in caves with thermal, hydrothermal, artesian, hypogene or mixed water origins, and they occur in caves which form through polygenetic processes; but are uncommon in stream caves.

In a hypogenic system, in contrast to an epigenic one, the various levels form almost contemporaneously: the lower storeys recharge and feed into the main system above through rising conduits. Laterally connected fractures in the bedrock may facilitate development of larger "master storeys" in the mid-levels of the system, whilst the upper levels are largely responsible for outflow. High cupola structures, sometimes with lateral extensions, may develop in the highest parts of the cave system (Klimchouk 2007, 2009). This description of a cave system underlain by a series of tubes and passages, with larger chambers developed in the (overlying) midsection and cupola developments present towards the very top, is reminiscent to that observed at Azokh Cave (Fig. 3.25).

After karst development ended, due to a lowering of the water table, the cave system was subsequently exposed and became accessible to animals and humans. As mentioned in the introduction, the cave is occupied by extremely large colonies of bats in the interior chambers of the cave system, and the evidence from excavation work in Azokh 1 passage suggests that they have resided there in large numbers for some time (Fernández-Jalvo et al. 2010; Sevilla 2016). At present, the most active speleogenic processes within the cave system appear to be those associated with the activities of bats, including their waste-products (guano and urine). Given the long amount of time they have been occupying the galleries, a considerable amount of guano has accumulated in the interior and these deposits have further modified the

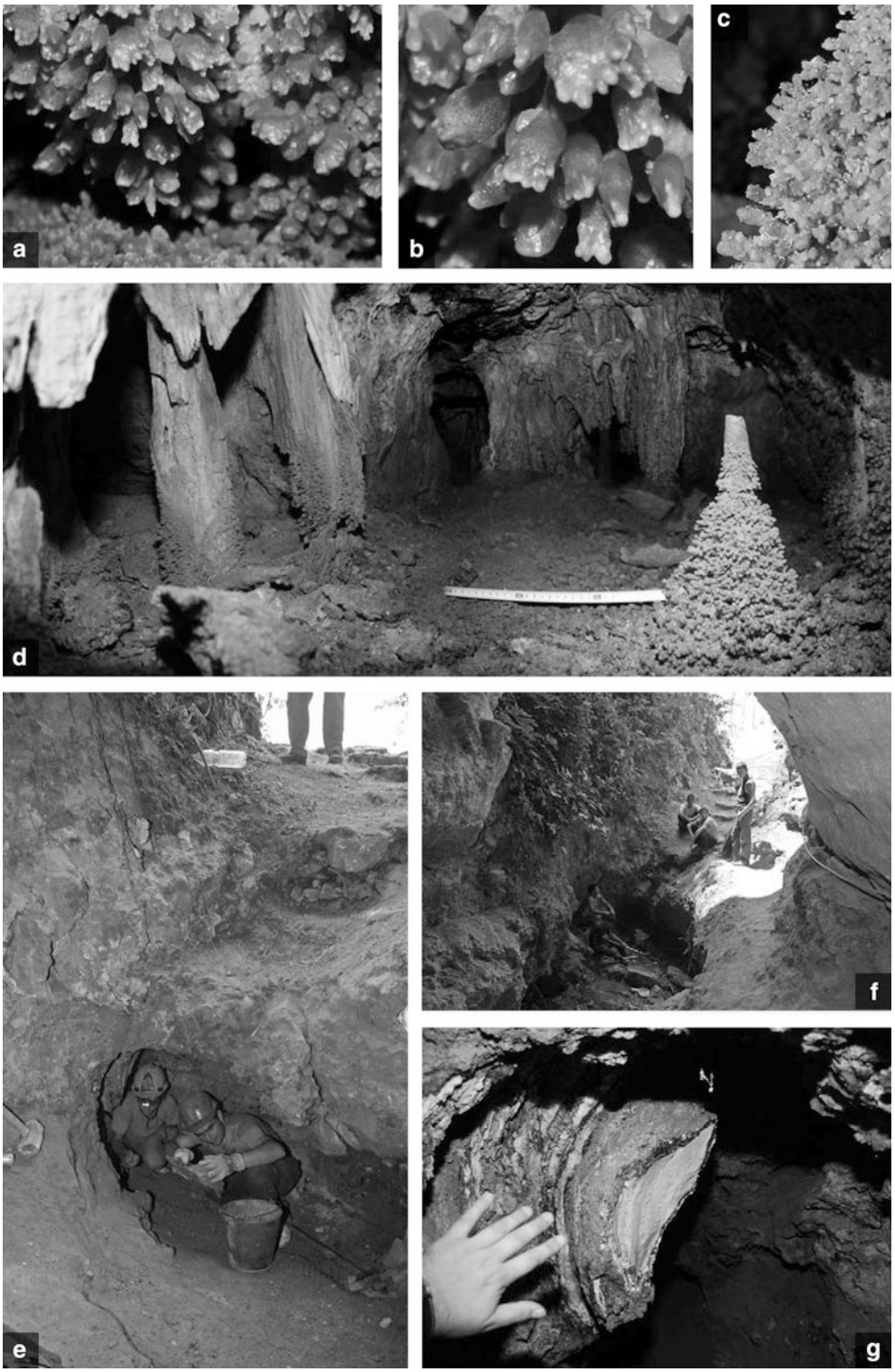

Fig. 3.23 The lowermost accessible gallery of the cave system at Azokh. **a**–**c** Detailed photographs of dogtooth calcite deposits which grew subaqueously; **d** General view of this lowermost gallery, as photographed the day it was discovered. Note the level of the watershed, as indicated by the upper limit of the dogtooth calcite development. The horizontal measuring tape is showing approximately 29 cm; **e**, **f** General views of the entrance to Azokh 1 passage showing the position of the lowermost gallery in the basal trench; **g** Speleothem found beneath the entrance to Azokh 1 passage. It is also visible immediately left of the helmet on person to left in (**e**). Access to the lowermost gallery was possible after excavating sandy sediments beneath this speleothem

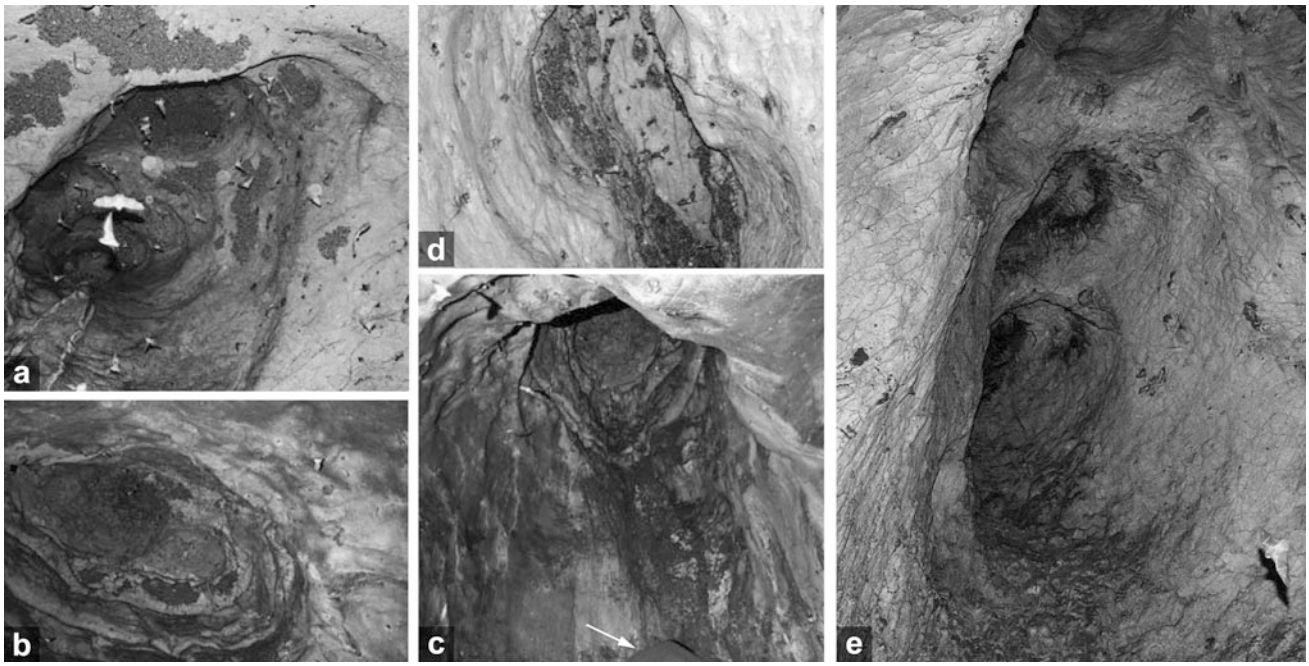

Fig. 3.24 Cupolas within the cave system at Azokh. **a** Cupola in the ceiling of the NE branch of Azokh I [*The Stalagmite Gallery*]; **b**, **c** Complex cupola in Azokh II [*The Sugar-mound Gallery*]. This is the largest cupola within the entire cave system and was formed by coalescence of a number of minor cupolas. In the very bottom of (**c**), the peak of a large mound of debris and bat guano is just visible (arrowed). This feature gives the gallery its name; **d**, **e** Elongated and complex (respectively) cupolas in the ceiling of Azokh IV [*The Hall Gallery*]

cave in a number of ways. Firstly, the heat from the guano pile helps to stimulate convective air flows in the cave atmosphere, and secondly, decomposition and alteration of this material produces a large amount of CO_2 and water vapor along with a number of strong, corrosive acids. These may then lead to biogenic corrosion, evident elsewhere, for example in the polygenetic Cuatro Ciénegas caves of Mexico (Piccini et al. 2007). At this particular site, large concave structures are developed in side walls; ceiling domes were generated due to condensation corrosion; and gullies and corrosion holes were produced in the floor of the cave due to the lowered pH of percolating fluids. In addition, condensation waters, enriched in salts, produced concretions and speleothems. Several of these features are also evident in the interior of Azokh Cave, and more importantly, where the modifying effect of bat guano is particularly strongly developed, it serves to obscure some of the original speleological features of the cave system, making interpretation problematic.

In summary, the multi-level, complex 3-dimensional morphology of the Azokh Cave system could be interpreted as epigenic, but also as hypogenic. A spongework cave pattern is not evident; instead cave formation is developed as a series of large, rounded galleries with interconnecting linear passages (Fig. 3.8). The change in cave pattern moving upwards through the limestone bedrock sequence (Fig. 3.25) makes interpretation complex. It is possible that most of the lower levels of the cave system formed in an epigenic regime; however, the upper levels may have had more of a hypogenic influence, leading to cupola and pendant formation. An additional issue is the general absence of speleothems inside of the cave, with the exception of the speleothem panel (Figs. 3.13d and 3.14a) and the large stalagmite (Fig. 3.13c) in Azokh I chamber and also the lowermost level beneath the entrance to Azokh 1 passage (Fig. 3.23). Clearly more investigation needs to be conducted to completely understand the origin of the cave; however, our preliminary interpretations indicate a complex, multifaceted history of formation and evolution.

◀ **Fig. 3.25** Plan views of cave development in the different layers (or levels) of the limestone bedrock at Azokh. **a** Passage development in the *Lower Limestone Unit*. Many of these are influenced by the trends of major joints and in some instances they meander; **b** The large main internal chambers or galleries are developed in the lower part of the *Upper Limestone Unit*; **c** Cupolas, collapse dolines, chokes and pits are developed in the upper part of the *Upper Limestone Unit*. The inset box in each image shows, in profile, the relative elevation of each type of cave development within the limestone sequence. The scale and north arrow on map (**a**) are also applicable to plan views (**b**) and (**c**)

Conclusions

1. A clear and detailed account of the geomorphology of the cave system at Azokh has been provided here for the first time. The cave formed from an abandoned karstic network developed in Mesozoic limestones and is composed of four large inner chambers (Azokh Galleries I–IV), which are laterally connected and arranged in a NW-SE trend. These are connected to the exterior via a series of NE-SW passages (Azokh 1, 5 and 6). These conduits all share a similar orientation with the regional pattern of jointing in the bedrock.
2. Doline collapse features figure prominently in the geomorphology of the cave. In the case of one of the entrance passages (Azokh 2), it has blocked access through to the inner galleries. Chert development within the limestone has had the opposite effect; in places it has served to stabilize and support ceiling structures, helping to reinforce and preserve various cave chambers.
3. The cross-sectional topography of the cave shows a higher central region (between inner chambers Azokh II and Azokh III), with a slope towards the two extremities of the cave system, although this descent is somewhat more pronounced towards Azokh 1 passage.
4. The thickness of the sediment infilling the various chambers may be determined from the electrical resistivity profiles, which have allowed the infill thicknesses to be mapped throughout the interior of the cave system. A variation in thickness is observed of <1 m to over 3 m. The greatest thicknesses of sediment occur in Azokh I, although there are also areas with elevated thicknesses at the entrance to Azokh II, along with more centralized areas in Azokh II, III and IV. A first order volume estimate of 1,367 m^3, based on a calculated surface area of approximately 1,390 m^2, was made for all the loose materials (sediment) lying on the surface of the limestone bedrock in the inner galleries at Azokh.
5. The geophysical profiles have identified several anomalies within the limestone bedrock, which, due to their morphology and resistivity values, probably represent cavities that are filled with fine materials. All the cavities that have been identified are associated in a general way with

conductive anomalies in the profiles that are interpreted as fractures. This confirms a relationship between fracture development, karstification and the formation of cavities.

6. It remains unclear whether the cave formed through epigenic or hypogenic speleological processes. This issue is further complicated by the presence of very large bat colonies in the interior of the cave system. The thick guano deposits generated by these creatures modify the inner galleries in a number of ways.

Acknowledgments We wish to thank the local people from Azokh Village for wholeheartedly supporting this endeavor, over a number of years and always making us feel welcome when we visit. In particular, Masis Ohanyan and Zorig Asryan very ably assisted us with the survey of the cave interior. The Royal Irish Academy is thanked for kindly granting permission to reproduce Fig. 3.1 (herein) from Murray et al. (2010). PDA, EA and JP acknowledge support from the Spanish Ministry of Science and Education (Projects BTE2000-1309, BTE2003-01552 and BTE 2007-66231).

References

Aracil, E., Maruri, U., Porres, J. A., & Espinosa, A. B. (2002). La tomografía eléctrica: una herramienta al servicio de la obra pública. *Rock Máquina, 76*, 30–34.

Aracil, E., Maruri, U., Vallés, J., Martínez Pagán, P., & Porres, J. A. (2003). Evaluación de problemas medioambientales mediante tomografía eléctrica. *Ingeopress, 122*, 34–39.

Brunet, M. F., Korotaev, M. V., Ershov, A. V., & Nikishin, A. M. (2003). The South Caspian Basin: A review of its evolution from subsidence modelling. *Sedimentary Geology, 156*, 119–148.

Cardozo, N., & Allmendinger, R. W. (2013). Spherical projections with OSXStereonet. *Computers & Geosciences*, *51*, 193–205.

David, E. (2008). *Visual Topo*. Available online at: http://vtopo.Free.fr.

Day, A. (2002). *Cave Surveying. Cave Studies Series 11*. Buxton: British Cave Research Association, 40 pp.

Dilek, Y., Imamverdiyev, N., & Altunkaynakc, Ş. (2009). Geochemistry and tectonics of Cenozoic volcanism in the Lesser Caucasus (Azerbaijan) and the peri-Arabian region: Collision-induced mantle dynamics and its magmatic fingerprint. *International Geology Review, 52*(4–6), 536–578.

Egan, S. A., Mosar, J., Brunet, M.-F., & Kangarli, T. (2009). Subsidence and uplift mechanisms within the South Caspian Basin: insights from the onshore and offshore Azerbaijan region. In M.-F. Brunet, M. Wilmsen & J. W Granath (Eds.), *South Caspian to Central Iran Basins* (Vol. 312, pp. 219–240). London: Geological Society (Special Publication).

Fernández-Jalvo, Y., Hovsepian-King, T., Moloney, N., Yepisko posyan, L., Andrews, P., Murray, J., et al. (2009). Azokh Cave project excavations 2002–2006: Middle-Upper Palaeolithic transition in Nagorno-Karabakh. Coloquios de Paleontología, Special Issue: Homage to Dr. D. Soria Madrid, Universidad Complutense de Madrid Press.

Fernández-Jalvo Y., King T., Andrews P., Yepiskoposyan L., Moloney N., Murray, J., et al. (2010). The Azokh Caves complex: Middle Pleistocene to Holocene human occupation in the Caucasus. *Journal of Human Evolution, 58*, 103–109.

Fossen, H. (2010). *Structural geology* (463 pp.). Cambridge: Cambridge University Press.

Gautam, P., Paj Pant, S., & Ando, H. (2000). Mapping of subsurface karst structure with gamma ray and electrical resistivity profiles: A case study from Pokhara valley, central Nepal. *Journal of Applied Geophysics, 45*, 97–110.

Griffiths, D. H., & Barker, R. D. (1993). Two-dimensional resistivity imaging and modelling in areas of complex geology. *Journal of Applied Geophysics, 29*, 211–226.

Gross, M. R., Fischer, M. P., Engelder, T., & Greenfield, R. J. (1995). Factors controlling joint spacing in interbedded sedimentary rocks: Integrating numerical models with field observations from the Monterey Formation, USA. In M. S. Ameen (Ed.), *Fractography: Fracture Topography as a Tool in Fracture Mechanics and Stress Analysis* (Vol. 92, pp. 215–233). Geological Society of London, Special Publication.

Huseinov, M. M. (1985). *The Early Palaeolithic of Azerbaijan (Kuruchai culture and stages of its development).* Baku (in Russian).

Kasimova, R. M. (2001). Anthropological research of Azykh Man osseous remains. *Human Evolution, 16*, 37–44.

Karakhanian, A. S., Trifonov, V. G., Philip, H., Avagyan, A., Hessami, K., Jamali, F., et al. (2004). Active faulting and natural hazards in Armenia, eastern Turkey and northwestern Iran. *Tectonophysics*, *380,* 189–219.

King, T., Compton, T., Rosas, A., Andrews, P. Yepiskoyan, L., & Asryan, L. (2016). Azokh Cave Hominin Remains. In Y. Fernández-Jalvo, T. King, L. Yepiskoposyan & P. Andrews (Eds.), *Azokh Cave and the Transcaucasian Corridor* (pp. 103–106). Dordrecht: Springer.

Klimchouk, A. B. (2007). *Hypogene Speleogenesis: Hydrogeological and Morphogenetic Perspective*. Special Paper no. 1, National Cave and Karst Research Institute, Carlsbad, NM, 106 pp.

Klimchouk, A. B. (2009). Morphogenesis of hypogenic caves. *Geomorphology, 106*(1–2), 100–117.

Lioubine, V. P. (2002). *L'Acheuléen du Caucuase*. ERAUL 93 Études et Recherches Archéologiques de l'Université de Liège. Liège.

Ljubin, V. P., & Bosinski, G. (1995). The earliest occupation of the Caucasus region. In Roebroeks, W. & van Kolfschoten, T. (Eds.), *The Earliest Occupation of Europe* (pp. 207–253). Leiden: University of Leiden.

Martínez-Pagán, P., Aracil, E., Maruri, U., & Faz, Á. (2005). Tomografía eléctrica 2D/3D sobre depósitos de estériles mineros. *Ingeopress, 138*, 34–36.

Mellors, R.J., Jackson, J., Myers, S., Gok, R., Priestley, K., Yetirmishli, G., et al. (2012). Deep Earthquakes beneath the Northern Caucasus: Evidence of Active or Recent Subduction in Western Asia. *Bulletin of the Seismological Society of America, 102,* 862–866.

Mosar, J., Kangarli, T., Bochudi, M., Glasmacher, U. A., Rast, A., Brunet, M-F., et al. (2010). Cenozoic–Recent tectonics and uplift in the Greater Caucasus: A perspective from Azerbaijan. In M. Sosson, N. Kaymakci, R. A. Stephenson, F. Bergerat & V. Starostenko (Eds.), *Sedimentary Basin Tectonics from the Black Sea and Caucasus to the Arabian Platform* (Vol. 340, pp. 261–279). London: Geological Society (Special Publications).

Mudrák, S., & Budaj, M. (2010). *The Therion Book*. Distributed under the GNU General Public License. 105 pp. Available online at: http://therion.speleo.sk.

Murray, J., Domínguez-Alonso, P., Fernández-Jalvo, Y., King, T., Lynch, E. P., Andrews, P., et al. (2010). Pleistocene to Holocene stratigraphy of Azokh 1 Cave, Lesser Caucasus. *Irish Journal of Earth Sciences, 28,* 75–91.

Murray, J., Lynch, E. P., Domínguez-Alonso, P., & Barham, M. (2016). Stratigraphy and Sedimentology of Azokh Caves, South Caucasus. In Y. Fernández-Jalvo, T. King, L. Yepiskoposyan & P. Andrews (Eds.), *Azokh Cave and the Transcaucasian Corridor* (pp. 27–54). Dordrecht: Springer.

Narr, W., & Suppe, J. (1991). Joint spacing in sedimentary rocks. *Journal of Structural Geology*, *13*, 1037–1048.

Osborne, R. A. L. (2004). The troubles with cupolas. *Acta Carsologica, 33*(2), 9–36.

Piccini, L., Forti, P., Giulivo, I., & Mecchia, M. (2007). The polygenetic caves of Cuatro Ciénegas (Coahuila, Mexico): Morphology and speleogenesis. *International Journal of Speleology, 36*(2), 83–92.

Porres, J. A. (2003). *Caracterización de cavidades en el subsuelo mediante la interpretación de perfiles de Tomografía Eléctrica: Aplicación al yacimiento arqueológico de Clunia.* Unpublished PhD Dissertation, University of Burgos, Spain. ISBN 978-84-96394-55-1.

Saintoti, A., Brunet, M.-F., Yakolev, F., Sébrier, M., Stephenson, R., Ershov, A., et al. (2006). The Mesozoic–Cenozoic tectonic evolution of the Greater Caucasus. In D. G. Gee & R. A. Stephenson (Eds.), *European Lithosphere Dynamics* (Vol. 32, pp. 277–289). London: Geological Society (Memoirs).

Sevilla, P. (2016). Bats from Azokh Caves. In Y. Fernández-Jalvo, T. King, L. Yepiskoposyan & P. Andrews (Eds.), *Azokh Cave and the Transcaucasian Corridor* (pp. 177–189). Dordrecht: Springer.

Sosson, M., Kaymakci, N., Stephenson, R., Bergerat, F., & Starostenko, V. (2010). Sedimentary basin tectonics from the Black Sea and Caucasus to the Arabian Platform: Introduction. In M. Sosson, N. Kaymakci, R. Stephenson, F. Bergerat & V. Starostenko (Eds.), *Sedimentary Basin Tectonics from the Black Sea and Caucasus to the Arabian Platform* (Vol. 340, pp. 1–10). London: Geological Society (Special Publication).

Sumanovac, F., & Weisser, M. (2001). Evaluation of resistivity and seismic methods for hydrogeological mapping in karst terrains. *Journal of Applied Geophysics, 47*, 13–28.

Vardanyan, M. (editor in chief) and others. (2010). *Atlas of the Nagorno-Karabakh Republic*. State Committee of the Real Estate Cadastre of the Nagorno-Karabakh Republic, Stepanakert, 96 pp.

Zhou, W., Beck, B. F., & Stephenson, J. B. (2000). Reliability of dipole-dipole electrical resistivity tomography for defining depth to bedrock in covered karst terrains. *Environmental Geology, 39*(7), 760–766.